Palaeogeography, Palaeoclimatology, Palaeoecology 670 (2025) 112939

Contents lists available at ScienceDirect

Palaeogeography, Palaeoclimatology, Palaeoecology

journal homepage: www.elsevier.com/locate/palaeo

Palaeoglacial and palaeoclimate inferences from cirque morphometry and spatial distribution across northern Patagonia (40° – 45° S)

R.L. Soteres [a,b,*], D.A. Cabrera [c], M.A. Martini [d], E.A. Sagredo [e,f], J. Pedraza [g], R.M. Carrasco [h], M.R. Kaplan [i], J.M. Araos [j]

[a] Centro de investigación GAIA-Antártica, Universidad de Magallanes, Punta Arenas, Chile
[b] Centro Internacional Cabo de Hornos (CHIC), Universidad de Magallanes, Puerto Williams, Chile
[c] Departamento de Geología, Universidad Andrés Bello, Santiago, Chile
[d] Centro de Investigaciones en Ciencias de la Tierra (CONICET), Facultad de Ciencias Exactas, Físicas y Naturales, Universidad Nacional de Córdoba, Córdoba, Argentina
[e] Instituto de Geografía, Pontificia Universidad Católica de Chile, Santiago, Chile
[f] Estación de Investigaciones Multidisciplinares Patagonia UC, Chile
[g] Departamento de Geodinámica, Estratigrafía y Paleontología, Universidad Complutense de Madrid, Madrid, Spain
[h] Departamento de Ingeniería Geológica y de Minas, Universidad de Castilla-La Mancha, Toledo, Spain
[i] Lamont-Doherty Earth Observatory, Columbia University, New York, USA
[j] Departamento de Geografía, Universidad de Chile, Santiago, Chile

ARTICLE INFO

Editor: Rebecca L. Totten

Keywords:
Cirque
Patagonia
Southern Westerly Winds
Morphometry
Glaciations
Palaeoclimate

ABSTRACT

The evolution of the cryosphere and climate in northern Patagonia during the late Pleistocene are relatively well-known thanks to chronologies on ice-marginal features. However, this knowledge mainly represents the magnitude and duration of extreme cold intervals occurring during glacial maxima. Consequently, less is known about the state of the glaciers and climate during transitions between full glacial and interglacial stages. Given that morphometric attributes of glacial cirques are considered as robust indicators of palaeoglacial and palaeoclimate conditions during phases of minor glaciation, examining cirques will yield key insights to assess the typology of glaciers and associated climate conditions during those pivotal periods. In this study, we systematically analyzed the morphology and spatial distribution of 3081 cirques in northern Patagonia between ~40° and ~ 45° S. Our findings revealed that circular cirques, reflecting widespread long-lived small glaciers, dominate northern Patagonia. Eastward increase of cirque floor altitude from the coast to the continent along with prevailing east-to-south aspects indicate a key role of westerly-controlled climate and radiative balance in cirque development. Morphometry and spatial distribution of cirques along with statistical analyses indicate that annual total precipitation, minimum temperature, and incoming solar radiation altogether play a major role in cirque development in northern Patagonia, although the relative importance of these factors might vary spatially. Regional lithology exerts a secondary influence mostly in cirque geometry. We conclude that the most frequent state of the cryosphere within the Pleistocene glacial cycles in northern Patagonia is characterized by moderate glaciations similar to that existing during glacial terminations.

1. Introduction

The Andes of Patagonia features widespread evidence of large-scale glaciations in southernmost South America since the Miocene (Mercer and Sutter, 1982; Rabassa et al., 2011; Clague et al., 2020). During the Last Glacial Maximum (LGM; ~33–18 ka; ka = 1000 years before present (BP); Denton et al., 1999a) an extensive ice body known as the Patagonian Ice Sheet (PIS) covered the Cordillera de los Andes from ~38° to ~56° S (Caldenius, 1932; Davies et al., 2020). This ice mass exhibited numerous outlet glacier lobes that left their geomorphic imprint on the landscape. In northern Patagonia (~40°-45° S), ice-marginal features, especially moraine ridges (Andersen et al., 1999; Garcia, 2012; Leger et al., 2020; Cooper et al., 2021; Soteres et al., 2022a), indicate that the PIS was dominated by piedmont glacier lobes that fluctuated recurrently during the LGM (Lowell et al., 1995; Denton et al., 1999a; Moreno et al., 2015). The evolution of the cryosphere in

* Corresponding author at: Centro de investigación Gaia Antártica, Universidad de Magallanes, Domo Antártico, Avda. Bulnes, 01855 Punta Arenas, Chile.
E-mail address: rodrigo.soteres@umag.cl (R.L. Soteres).

https://doi.org/10.1016/j.palaeo.2025.112939
Received 11 July 2024; Received in revised form 20 February 2025; Accepted 5 April 2025
Available online 19 April 2025

northern Patagonia during Termination 1 (T1; ~18–11.7 ka; Denton et al., 2010) is based on few glacial chronologies and numerical modelling that point to a rapid disintegration of the PIS leading to smaller glaciers at the headwalls of the southern Andes between ~18–16 ka (Leger et al., 2021; Moreno et al., 2022; Soteres et al., 2022b; Cuzzone et al., 2024). This behavior suggests that glaciers in this portion of the PIS might be particularly sensitive to climate variations (Sagredo and Lowell, 2012; Sagredo et al., 2014; Caro et al., 2021; Yan et al., 2022). However, the drivers that influenced Patagonian glaciers during deglacial intervals and outside glacial maxima between of interglacial states remains largely unknown. Recognizing these controlling factors through empirical evidence will contribute to deciphering the mechanisms that potentially drove past climate variability and former cryosphere during much of the glacial-interglacial cycles of the Pleistocene in the middle latitudes of the southern hemisphere.

Cirques are ubiquitous erosional landforms of glacial origin widely distributed across mountain ranges around the planet (Barr and Spagnolo, 2015a). Despite their great variability in size and shape, cirques often appear as semicircular hollows delineated by steep headwalls and open thresholds featuring marked changes in the slope down valley, which is occasionally closed by moraine ridges (Fig. 1; Evans and Cox, 1974). Cirques are thought to form by enhanced subglacial/glacial erosion that excavate and enlarge pre-existing mountain depressions when the ice is constrained by the local topography (Barr et al., 2019; Crest et al., 2017). For this reason, they have been traditionally considered as indicators of past glacier dynamics and climate variability during early and final stages of full glaciation episodes (Barr and Spagnolo, 2015a). This implies that cirque morphology is a robust proxy to assess the evolution of the former cryosphere and climate conditions between glacial maxima and interglacial intervals coinciding with less-extensive glaciations (Porter, 1989). In addition, cirques offer a unique opportunity to conduct geomorphic-based palaeoclimate reconstructions in remote locations and/or areas with poorly preserved ice-marginal landforms, such as the headwalls of the northern Patagonian Andes.

Cirques have been recognized as singular features across former glacierized landscapes since the 19th century (de Charpentier, 1823) and a major source of palaeoenvironmental information since the early 20th century (Brown, 1905). Systematic analysis of cirques has grown profusely in past decades (Evans and Cox, 1974; Evans, 1977). To date, comprehensive analyses of cirque morphometric attributes have been conducted mostly in the mid-to-high latitudes of the Northern Hemisphere, such as in numerous mountain ranges in North America, including the Cascade Range (Porter, 1977) and many more sumarized by Evans (1977), Iceland (Ipsen et al., 2018; Principato and Lee, 2014), Britain and Ireland (corries, cwm; e.g., Barr et al., 2017, 2019), the Iberian Peninsula (e.g., García-Ruiz et al., 2000; Delmas et al., 2014, 2015; Crest et al., 2017; Pellitero et al., 2024), the Alps (e.g., Federici

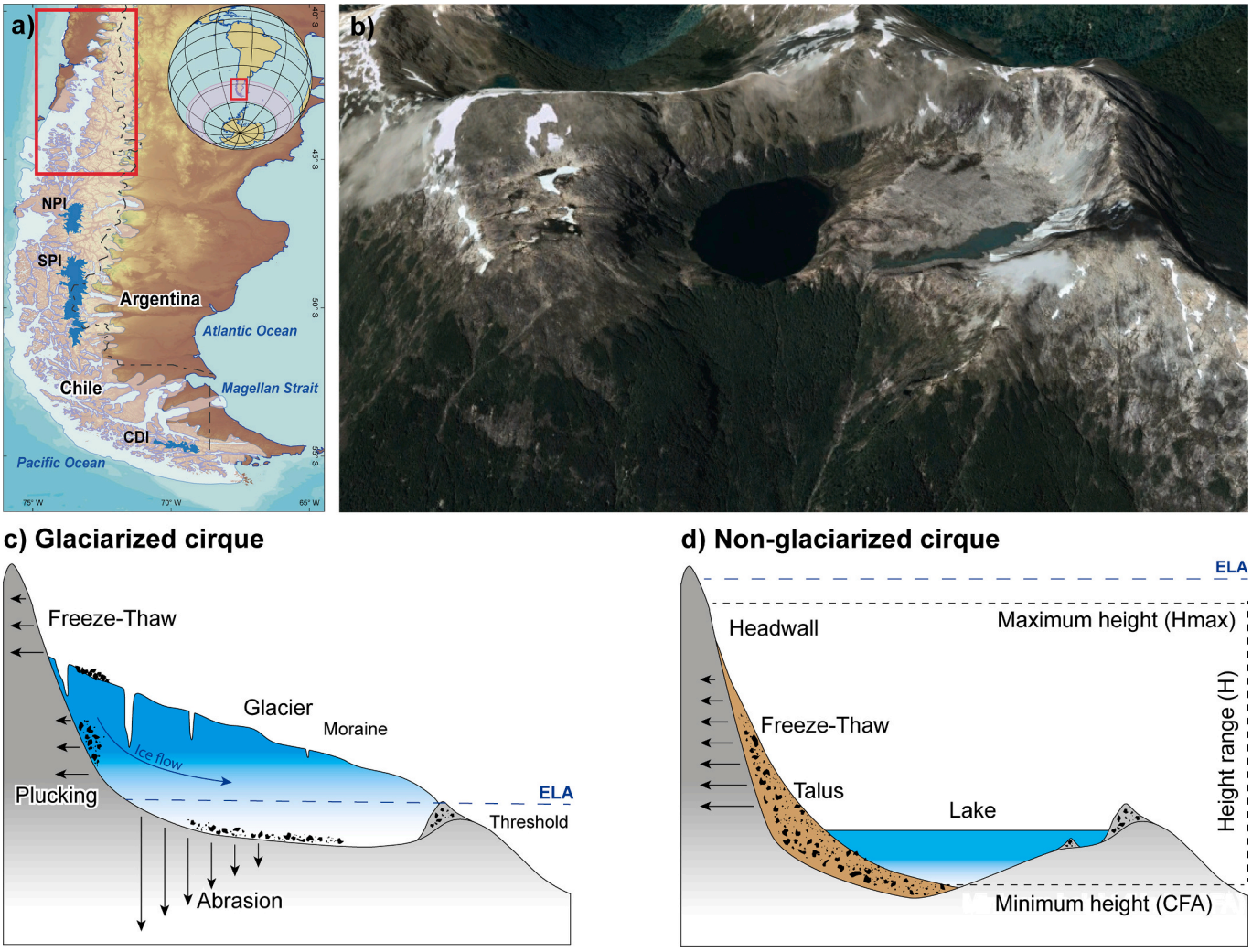

Fig. 1. Location map of the study area. a) Main map presents the extent of the PIS at 35,000 years BP during the LGM (Davies et al., 2020; white polygon) and the present-day Northern (NPI) and Southern (SPI) Patagonian Icefields and the Cordillera Darwin Icefield (CDI). b) Example of glacial cirque in northern Patagonia (Google Earth image). c) and d) Idealized models of geomorphic processes occurring in glaciarized and non-glaciarized cirques.

and Spagnolo, 2004; Anders et al., 2010), the mountains of Greece (e.g., Hughes et al., 2007; Bathrellos et al., 2014), Carpathian mountains (e.g., Mîndrescu et al., 2010; Křížek and Mida, 2013; Ruszkiczay-Rüdiger et al., 2021), the Scandinavian Peninsula (e.g., Oien et al., 2020, 2022), the Anatolian-Caucasus mountains (e.g., Simsek et al., 2023), major Asian mountain ranges (e.g., Zhang et al., 2020, 2021; Li et al., 2023) and the Kamchatka Peninsula (Barr and Spagnolo, 2013, 2015a). Conversely, cirques in the Southern Hemisphere have received significantly less attention (Brook et al., 2006; Araos et al., 2018; Oliva et al., 2020; Barr et al., 2022; Barr et al., 2024).

Even after decades of scientific efforts towards deciphering past glacial and palaeoclimate conditions in Patagonia (e.g., see Soteres et al., 2023), research focused on cirques is surprisingly scarce in the region. Pioneer studies investigated small cirque populations within constrained areas of southern Patagonia and Tierra del Fuego, specifically in Sierra Baguales (~50°-51° S; Araos et al., 2018) and the Vinciguerra-Sorondo ranges in Tierra del Fuego (~54.5° S; Oliva et al., 2020), respectively. Hence, their representativeness as palaeoglacial and/or palaeoclimate state likely is mostly local, precluding our ability to further interpret Patagonian cirques as indicators of past glacial and climate evolution at a large spatial scale.

Northern Patagonia is an ideal location for studying cirques because it is one of the least glacierized mountain areas of the southern Andes and, therefore, features a high number of well-preserved currently ice-free cirques (Glasser et al., 2008; Glasser and Jansson, 2008). Furthermore, the position of these landforms coincides with the northernmost portion of the PIS during the last and prior glaciations (Denton et al., 1999a; Thomson et al., 2010; Leger et al., 2023) and, thus, they geographically span a particularly climate-sensitive section of the former ice body. Here, we present a regional inventory of cirques located at the core of the northern Patagonia Andes (~40°-45° S) spanning from the Pacific Ocean to the inland continental steppes. In addition, we perform quantitative analyses of their morphometric attributes and spatial distribution to explore their links with regional geology and present climatic conditions to assess their suitability as palaeo -glacial and -climate proxies. Consequently, we aim to contribute new insights to better understand the magnitude and dynamics of past glaciations and climate in the middle latitudes of the Southern Hemisphere.

2. Regional setting

In this study, we focus on the cirques distributed in northern Patagonia that extend across the southern Andes in South America between ~40° - 45° S and ~ 74.5° -70° W, including Chilean and Argentinean territory (Fig. 1).

From west to east, the study area spans from the Pacific Ocean to the interior steppes (i.e., pampas), including the Cordillera de los Andes, also referred as the Patagonian Andes. The regional geology is dominated mainly by Paleozoic metamorphic lithologies in the Cordillera de la Costa and the Pacific islands to the west, including Isla Grande de Chiloé and Archipiélago de las Guaitecas, followed by the Jurassic-Neogene North Patagonia Batholith dominating the spine of the main Patagonian Andes and Jurassic volcanic rocks with alternating sedimentary sequences to the east (Supplementary material). Quaternary lithologies mainly composed of glacial and fluvioglacial deposits are mostly restricted to the lee side of the Cordillera de la Costa, valley floors of the principal Cordillera de los Andes and eastern steppes (Lizuaín and Panza, 2018; SERNAGEOMIN, 2003). Tectonically, northern Patagonia is traversed by the Liquiñe-Ofqui fault zone, which consists of a north-to-south trending strike-slip major crustal discontinuity (Cembrano et al., 1996). This faulting system partially controls the regional volcanism resulting in the Southern Andean Volcanic Zone (Pérez-Flores et al., 2016). Recent studies in northern Patagonia based on geomorphic-sedimentary assemblages, geochronologic data and numerical modelling have addressed regional glaciovolcanism during the past 100 ka (Singer et al., 2024).

At present, seasonal temperatures and, especially, precipitation (Fig. 2a, b, c) in Patagonia relate closely to low-level zonal winds, indicating that Southern Westerly Winds (SWW) and associated atmosphere-ocean climate components are the major drivers of regional climate (Garreaud et al., 2013). Therefore, the annual latitudinal displacement of the SWW and the orographic effect exerted by the Patagonian Andes play a key role in controlling regional precipitation and temperature (Garreaud et al., 2013). In the north portion of northern Patagonia, from west to east, data collected in meteorological stations clearly capture a strong rain-shadow effect ranging from ~1830 mm/yr close to the coast of the Pacific Ocean (Puerto Montt, ~41.5° S, 90 m asl), to ~745 mm/yr in the foot of the eastern flank of the austral Andes (San Carlos de Bariloche, ~41° S, 846 m asl). In the central portion of the region, the precipitation reaches values of ~3615 mm/yr near the Pacific coast (Chaitén, ~42.9° S, 10 m asl), to ~430 mm/yr in the Argentinean plains (Esquel, ~42.9° S, 799 m asl). Finally, in the southern sector of the study area, precipitation ranges from ~2460 mm/yr to the west (Puerto Aysén, ~45.4° S, 8 m asl), to ~335 mm/yr to the east (Coyhaique Alto, ~45.6° S, 730 m asl). Although less pronounced, there is also an eastwards variation in temperature annual range from ~10° to ~15° C depending on the latitude of the study area (data retrieved from www.explorador.cr2.cl).

3. Materials and methods

We identified cirques with less than ~10 % of glacier coverage in northern Patagonia from ESRI Imagery (SPOT ~2.5 m spatial resolution) and digital elevation model ALOS PALSAR (DEM; ~12.5 m spatial resolution) following the criteria first outlined by Evans and Cox (1974) and after revised in Barr and Spagnolo (2015a) and Evans and Cox (2017). Accordingly, we delimited cirque polygons by outlining the crest of the headwalls exhibiting slopes >27° that enclose relatively flat bottoms of <20° (Fig. 3). This mapping criteria matches prior cirque morphometric analysis in Patagonia (Araos et al., 2018; Oliva et al., 2020). Subsequent mapping was carried out in ArcGIS 10.4 software. We cross-checked our cirque inventory with prior glacial geomorphic studies in the region (Glasser et al., 2008; Glasser and Jansson, 2008; Davies et al., 2020).

We extracted cirque morphometric parameters using the ArcGIS add-in Automated Cirque Metric Extraction (ACME) (Spagnolo et al., 2017). Subsequently, we compiled metrics regarding the cirque geometry: length (L; meters), width (W; m), height range (H; m). Then, we described cirques shape according to L/W, L/H, W/H ratios and the circularity index. L/W ratio measures the planimetry of the cirques with values closer to 1 suggesting circular shapes, while higher values point to increased elongation. L/H and W/H are often interpreted as a measure of cirque vertical incision with low values suggesting strong incision (Barr and Spagnolo, 2015b). Circularity index corresponds to the ratio between the perimeters of a certain cirque and a circle of the same area, indicating maximum circularity when it is closer to 1. Finally, we assessed the size parameter using the equation $\sqrt[3]{LWH}$ which reflects an isometric development (i.e., homogeneous enlargement) when the power regression values of the L, W and H against the size are equal, in contrast to an allometric evolution (i.e., heterogeneous enlargement) when the power regression values differ each other (Evans, 2006a). We also obtained information regarding the spatial distribution of the cirques, such as latitude (°), longitude (°) and distance to the coast (DTC; km). DTC was calculated using the Near tool of ArcGIS 10.4 (Oien et al., 2020). We emphasized cirque floor altitude (CFA; m asl), equating to the minimum elevation of the cirque, because it is a suitable indicator of past glacial equilibrium line altitude (ELA; Benn and Lehmkuhl, 2000; Porter, 2001). Finally, we extracted basic topographical parameters of the cirques such as the mean slope (Smean; degrees) and the mean aspect (Amean; degrees). The former is calculated by averaging the slope value of every pixel within the cirques and the latter by averaging

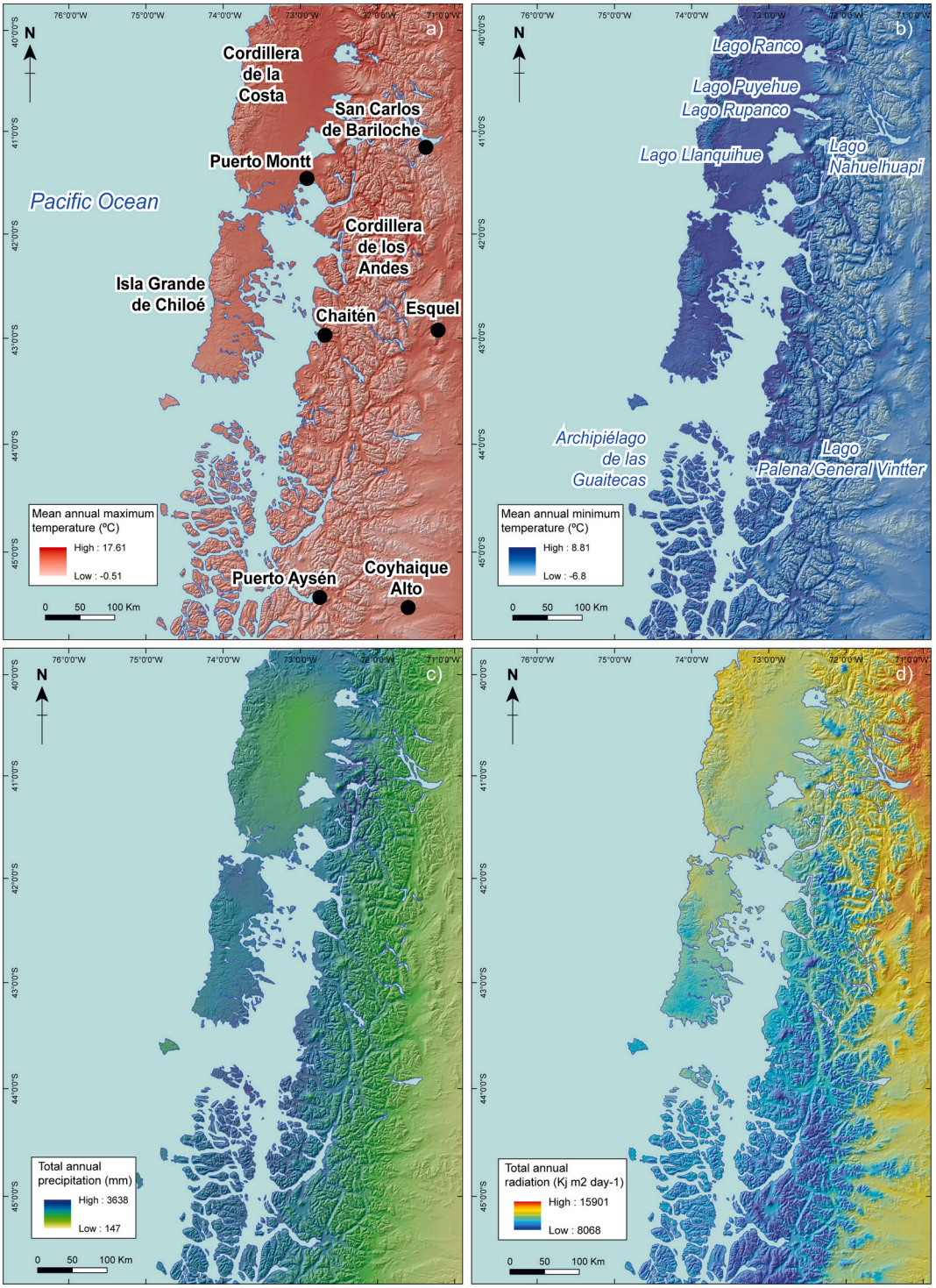

Fig. 2. Present-day climate maps of northern Patagonia for the period 1970–2000 (Fick and Hijmans, 2017). a) Annual mean maximum temperatures (°C); b) Annual mean minimum temperatures (°C); c) Annual total precipitation (mm); d) Annual total radiation (kj m2 day^{-1}).

the arctangent of the ratio between mean sine and mean cosine from every radian-converted pixel aspect within cirques (Spagnolo et al., 2017).

Based on statistical analysis, we explored links between the cirque attributes and regional climate and geology using MATLAB 2017 software. First, to conduct intrapopulation comparison, we performed a k-means clustering analysis considering the circularity and L/W indices, which are commonly interpreted as an indicator of the glaciation style in terms of magnitude (Barr and Spagnolo, 2015a). Second, we implemented CircStats toolbox (Berens, 2009) to analyze circular statistics of the cirque aspects, such as vector mean and strength (Evans, 2006b). Third, we assume that regional present-day climate patterns are analogous to those in the past but different in magnitude (Rojas et al., 2009), so we performed multivariate Pearson correlation and principal component analysis (PCA) to assess the relationship between modern climate variables and cirque attributes, including annual, summer and winter mean maximum and minimum temperatures (°C), annual mean radiation (Kj m^2 day^{-1}) and annual total precipitation (mm). Climate

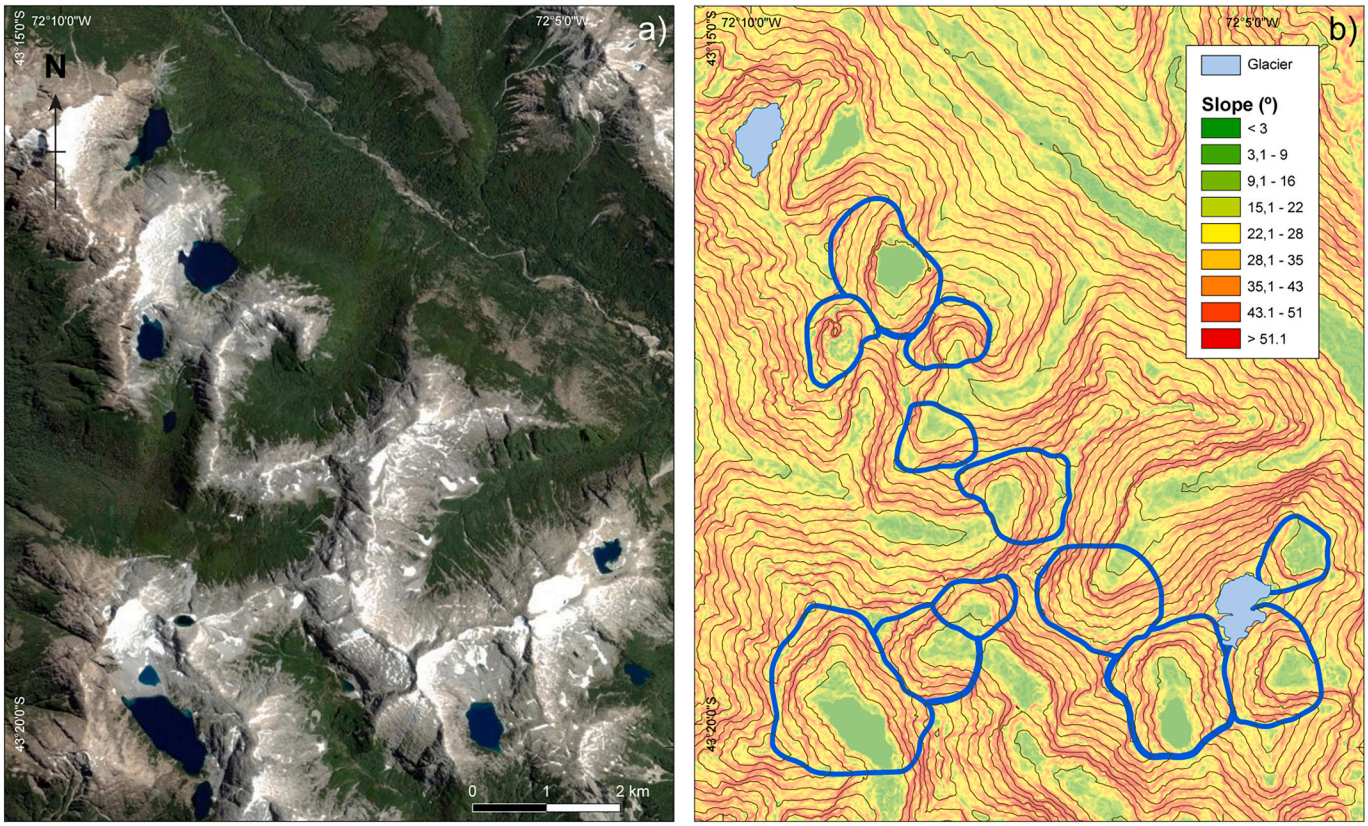

Fig. 3. Examples of cirques in northern Patagonia mapped in this study. a) Satellite image from ESRI Imagery. b) Slope model extracted from ALOS Palsar DEM depicting mapped cirques (blue polygons). Contour lines are shown as thin dark lines. (For interpretation of the references to colour in this figure legend, the reader is referred to the web version of this article.)

data was collected from the WorldClim V2 (Fig. 2; 1 km spatial resolution; Fick and Hijmans, 2017). Fourth, we conducted one-way analysis of variance (ANOVA) to investigate potential correlations between regional geology and cirque morphometry and spatial distribution (e.g., Barr et al., 2017). Main lithological units in northern Patagonia were compiled in a first-order map (Supplementary material) from the 1:1.000.000 scale geological map published by the Chilean Servicio Nacional de Geología y Minería (SERNAGEOMIN, 2003) and the 1:2.500.000 geological map produced by the Argentina Servicio Geológico Minero Argentino (Lizuaín and Panza, 2018). Additionally, to assess the influence of regional topography on cirque distribution, we performed a swath profile covering the study area with the ArcGIS add-in SwathProfiler (Pérez-Peña et al., 2017).

4. Results

We mapped a total of 3081 cirques widely distributed across northern Patagonia between ~40° -45° S and ~ 74.5° -70° W. We did not identify any cirque in Cordillera de la Costa between its continental portion and Isla Grande de Chiloé north of ~44° S (Fig. 4). We argue that if glaciers ever existed in the Chilotan Cordillera de la Costa, their geomorphic imprint is either obscured by the forest or has been deeply altered, leading to significant uncertainties when differentiating glacial from fluvial landforms We distinguished more cirques than prior mapping efforts in northern Patagonia, particularly in the Archipiélago de las Guaitecas (Glasser et al., 2008; Glasser and Jansson, 2008). This is most likely due to recent improvements in the spatial resolution of satellite imagery and DEMs, which may have limited cirque detection in earlier studies, especially in low-elevation mountain ranges and densely vegetated areas along western Patagonia in Chile. Cirques vary in preservation, sometimes hampering identification, so we consider this population to represent a minimum estimate of the total number of cirques in the region.

4.1. Cirque geometry in northern Patagonia

Cirques in northern Patagonia exhibit on average a length of 1100 ± 469 m, a width of 1107 ± 438 m and a height of 500 ± 204 m (Table 1). The mean size value reaches 836 ± 311 m. The circularity index of the entire population is 1.06 ± 0.42 and the L/W index is 1.02 ± 0.28, both indicating circular plan form. Vertical incision indices L/H and W/H are 2.30 ± 0.75 and 2.36 ± 0.72, respectively, suggesting relatively intense deepening processes on cirque evolution (Table 2).

The k-means clustering analysis identifies two groups of cirques delimited by the parallel ~43° S (Supplementary material), which will serve for intrapopulation comparisons. The northernmost and southernmost regions of northern Patagonia feature 1402 and 1679 cirques, respectively. On average, cirques of the northern group present 1048 ± 433 m in length, 1070 ± 404 m in width, and 494 ± 203 m in height, whereas the southern sector present respective metrics of 1144 ± 493 m, 1138 ± 463 m and 504 ± 206 m (Table 1). Mean size values (Evans, 2006a) of the northern and southern subpopulations are 810 ± 292 m and 857 ± 324 m, respectively. Overall, southern cirques present a slightly larger size and higher variability than their northern counterparts. The mean circularity index and mean L/W ratio are 1.06 ± 0.37 and 0.99 ± 0.26, respectively, for the cirques of the northern sector, while the southern sector reveals equivalent metrics of 1.07 ± 0.44 and 1.03 ± 0.29, respectively. This suggests that the entire population of cirques in northern Patagonia exhibits circular plan forms. On average, vertical incision indices L/H and W/H for the northern subpopulation are 2.22 ± 0.73 and 2.29 ± 0.68, while for the southern subpopulation correspond to 2.36 ± 0.76 and 2.37 ± 0.76, suggesting that northern

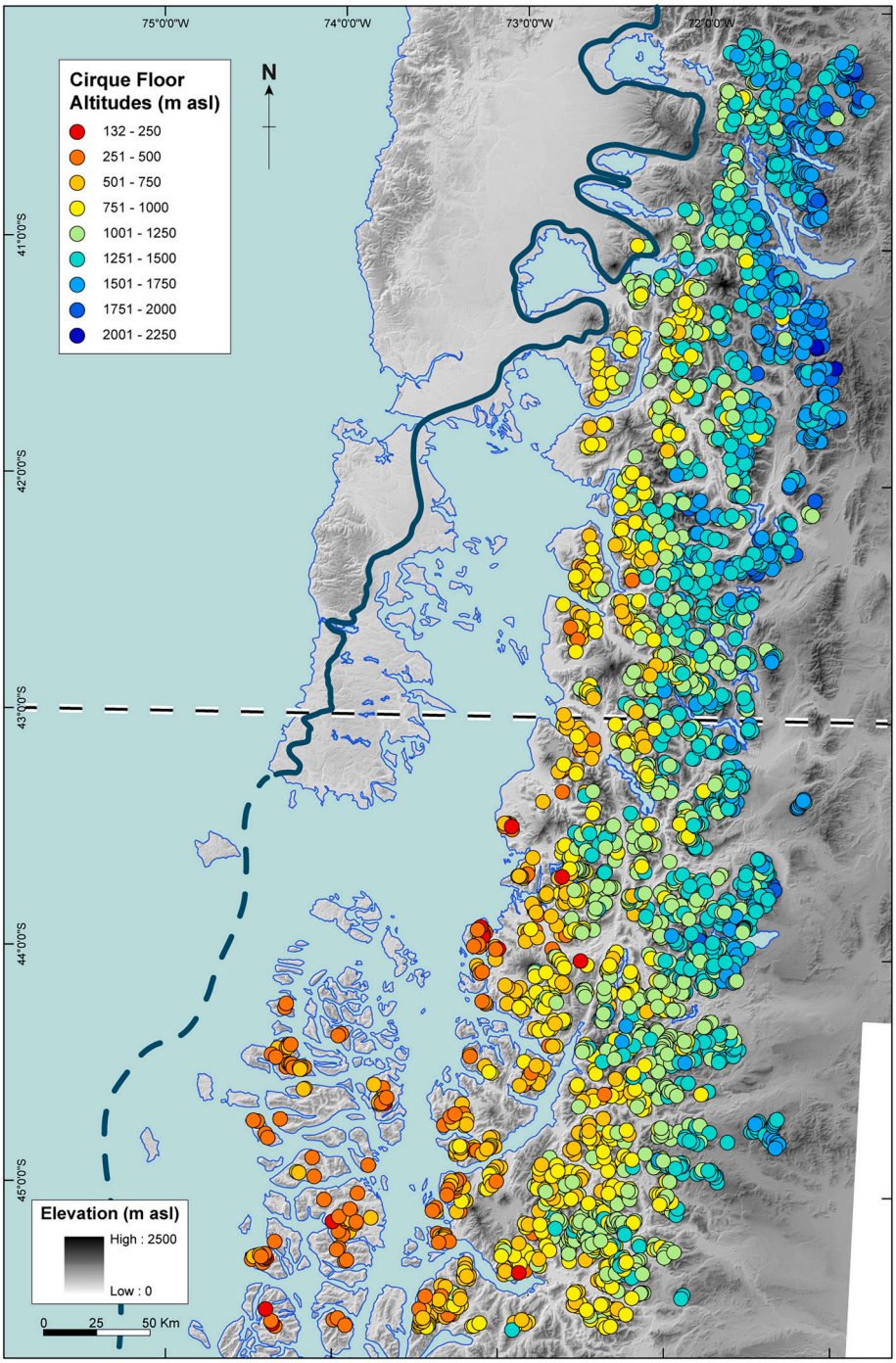

Fig. 4. Distribution of cirques and CFA (cirque floor altitudes) in northern Patagonia (n = 3081). Blue line corresponds to the LGM limit of the PIS according to Denton et al. (1999a), Garcia (2012), Davies et al. (2020) and Soteres et al. (2022a). (For interpretation of the references to colour in this figure legend, the reader is referred to the web version of this article.)

cirques tend to present a slightly larger vertical development than their southern counterparts (Table 2).

Assessment of isometry/allometry development of the cirques based on the sum of exponents of the logarithms of L, W and H plotted against the logarithm of size (Delmas et al., 2015) yield exponent values of 1.04, 0.92 and 1.04 for the northern subpopulations, whereas for the southern subpopulations are 1.03, 0.98 and 0.99. (Fig. 5).

4.2. Altitudinal distribution of cirques in northern Patagonia

The mean cirque floor altitudes (CFA) in northern Patagonia (Fig. 4) differ between subpopulations ranging from 1326 ± 300 m asl and 1032 ± 356 m asl, in the northern and southern sectors, respectively (Table 3). Overall, CFA gradually decreases poleward and increases eastwards (i.e, inland). In latitude, northern cirques CFA vary linearly from ~1500 m asl in Lago Ranco (~40° S) to ~1200 m asl in Chaitén (~43° S; r^2 = 0.15), whereas CFA of southern cirques span between ~1200 m asl in Chaitén and ~ 800 m asl in Coyhaique (~45° S; r^2 = 0.13; Fig. 6a). In longitude, CFA in the mainland increases linearly, although the CFA of the whole population seems to rise exponentially from the coast to the continent. Northern cirques are distributed along the southern Andes between ~750 m asl close to the western shore of Lago Rupanco and ~

Table 1
Descriptive statistics for main geometrical attributes of cirques in northern Patagonia.

	All cirques				Northern sector cirques				Southern sector cirques			
	L (m)	W (m)	H (m)	Size (m)	L (m)	W (m)	H (m)	Size (m)	L (m)	W (m)	H (m)	Size (m)
Max	4168	3265	1420	2549.92	3896	3053	1403	1947.70	4168	3265	1420	2280.92
Min	191	211	64	182.20	191	310	90	193.84	258	211	64	182.20
Mean	1100.23	1106.99	499.62	835.98	1048.30	1069.63	493.90	810.37	1143.60	1138.18	504.40	857.37
Sdev	468.71	438.13	204.36	311.07	432.93	403.90	202.69	292.42	492.69	462.60	205.75	324.37
Skew	1.07	1.01	0.82	0.81	1.03	1.06	0.83	0.76	1.05	0.93	0.82	0.81
10th Percentile	577.20	615.40	265	472.59	562.70	619	264	469.58	593.40	612	267	473.68
90th Percentile	1731.80	1677	775.80	1251.73	1630.20	1610.90	774.60	1209.33	1812.60	1756.80	778.60	1276.70

Table 2
Descriptive statistics for shape attributes of cirques in northern Patagonia.

	All cirques				Northern sector cirques				Southern sector cirques			
	Circ	L/W	L/H	W/H	Circ	L/W	L/H	W/H	Circ	L/W	L/H	W/H
Max	1.37	2.78	11.60	10.39	1.32	2.41	10.38	6.57	1.37	2.78	11.56	10.39
Min	1.01	0.37	0.83	0.67	1.01	0.37	0.83	0.68	1.01	0.37	0.90	0.67
Mean	1.06	1.02	2.30	2.36	1.06	0.99	2.22	2.29	1.07	1.04	2.36	2.37
Sdev	0.42	0.28	0.75	0.72	0.37	0.26	0.73	0.68	0.44	0.30	0.76	0.76
Skew	1.79	0.97	2.16	1.60	1.70	0.90	2.10	0.97	1.77	0.99	2.22	1.94
10th Percentile	1.03	0.70	1.51	1.54	1.02	0.69	1.47	1.53	1.03	0.70	1.56	1.55
90th Percentile	1.12	1.39	3.21	3.25	1.11	1.34	3.08	3.18	1.13	1.42	3.27	3.35

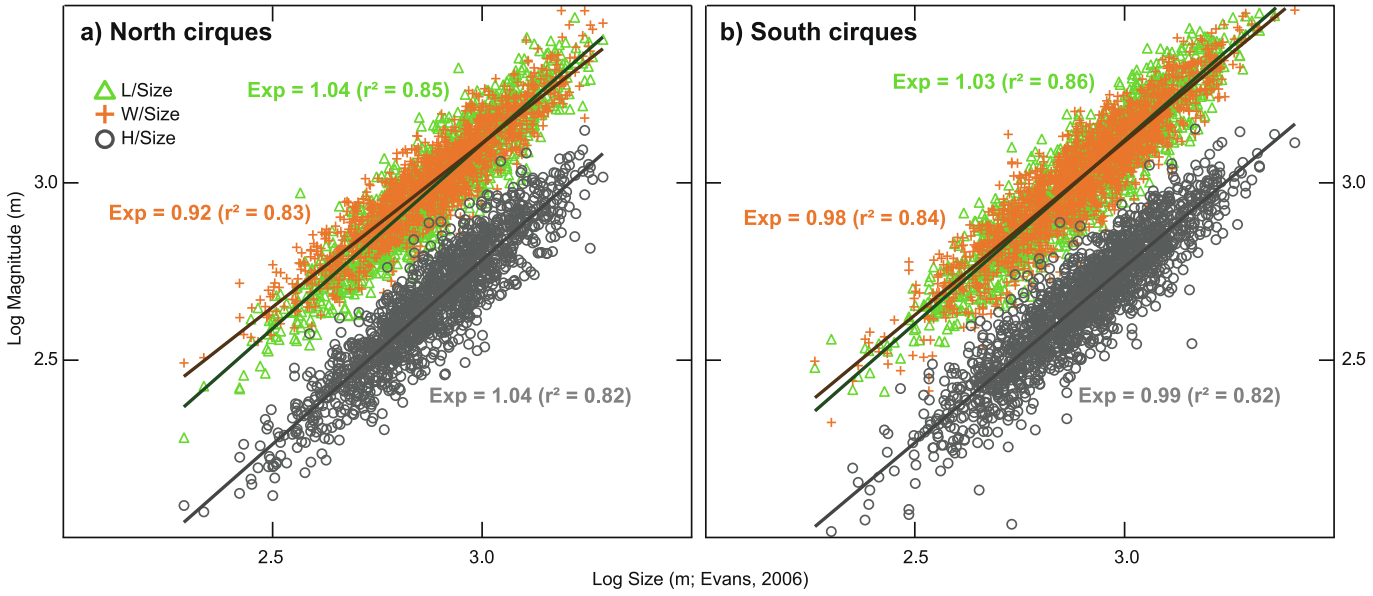

Fig. 5. Plots of length (L), width (W) and altitudinal range (H) logarithms against size logarithms for a) northern and b) southern subpopulations. Power exponents and r2 are shown in the colour of each variable.

Table 3
Descriptive statistics for altitudinal attributes of cirques in northern Patagonia.

	Northern sector cirques			Southern sector cirques		
	CFA (m asl)	Hmax (m asl)	Hmean (m asl)	CFA (m asl)	Hmax (m asl)	Hmean (m asl)
Max	2052	2475	2202	1807	2211	1939
Min	280	1019	613	132	584	373
Mean	1326.06	1819.96	1558.10	1032.27	1536.67	1265.29
Sdev	300.13	255.90	262.59	335.93	315.49	309.43
Skew	−0.44	−0.58	−0.57	−0.37	−0.70	−0.59
10th Percentile	912.60	1466.90	1174	547	1051	780
90th Percentile	1679.70	2120.70	1863.70	1439	1890	1629

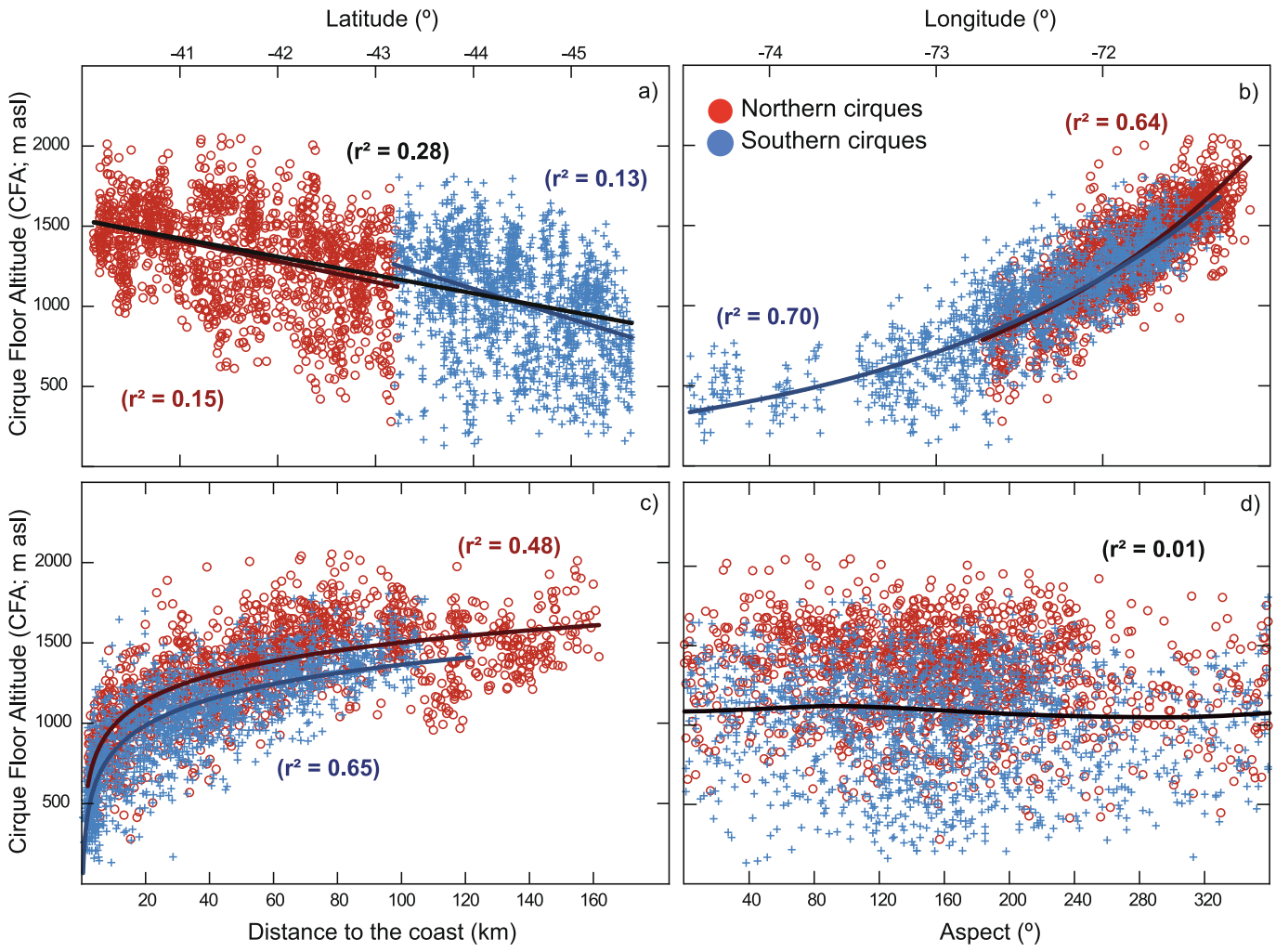

Fig. 6. Variation of cirque floor altitude in northern Patagonia against a) latitude; b) longitude; c) distance to the coast and d) aspects. Red dots and blue crosses are the northern and southern subpopulations, respectively. Solid lines represent the main cirque trendline of each subregion. (For interpretation of the references to colour in this figure legend, the reader is referred to the web version of this article.)

1900 m asl in the surroundings of Lago Nahuelhuapi (r^2 = 0.64), whereas southern cirques are dispersed between Archipiélago de las Guaitecas (~44° S) and the Patagonian Andes, including some minor secondary ranges of the eastern flank, between average elevations of ~400 and ~ 1500 m asl (r^2 = 0.70; Fig. 6b). Regionally, CFA sharply increases inland in the first kilometers from the coast following a logarithmic trend (Fig. 6c). In the northern subregion there are no cirques close to the Pacific coast north of ~44° S. On the contrary, south of this latitude, cirques rise rapidly from the Chilotan Interior Sea towards the Patagonian Andes (r^2 = 0.48), whereas the rising of cirques in southern subregion is more subtle because of the tens of cirques in the low islands of Archipiélago de las Guaitecas before reaching continental mountains (r^2 = 0.65). Finally, the majority of cirques between ~500 to ~1750 m asl of elevations present aspects ranging between ~80° and ~ 240°. Fourier regression of aspects and CFA of the whole cirque population indicates no significant correlation between CFA and dominant aspects (r^2 = 0.01; Fig. 6d).

4.3. Topographical parameters of cirques in northern Patagonia

The northern and southern groups of cirques feature similar slopes with mean values of 29.36° (range: 11°-46 °) and 28.40° (range: 8°-48°), respectively (Supplementary material).

Cirques in northern Patagonia exhibits a vector mean of 147.62° accounting for a dominant SE-SSE orientation with a vector strength of 41 %. Cirques from the northern and southern subpopulations exhibit similar dominant aspects with vector means of 147.35° and 147.89° and vector strengths of 42 % and 39 %, respectively (Fig. 7). Overall, cirques present a marked asymmetry with a frequent combination of poleward and inland aspects.

4.4. Regional present-day climate and cirque attributes in northern Patagonia

Taking together the whole population of cirques in northern Patagonia, Pearson correlation matrices reveal weak correlations between present-day climate variables and cirque attributes such as L, W and geometry indices ($r < 0.2$; Table 4). Northern Patagonian population of cirques exhibit strong correlations between CFA and some climate variables and climate-modulating geographic parameters, such as annual mean minimum temperatures (Tmin; $r = -0.86$), annual total precipitation (Precip; $r = -0.84$) and longitude (Long; $r = 0.84$; Table 5). Also, it is worth mentioning the good correlation observed between CFA and distance to the coast (DTC; $r = 0.71$), latitude (Lat; $r = 0.53$), incoming solar radiation (Rad; $r = 0.48$) and annual mean maximum temperatures (Tmax; $r = -0.36$; Table 5). Pearson correlations between CFA and seasonal temperatures feature high correlation with mean winter (June–July-August) temperatures (Tmean winter; $r = -0.74$; Supplementary material) and moderate with mean summer (December–January-February) temperatures (Tmean summer; $r = -0.46$). We

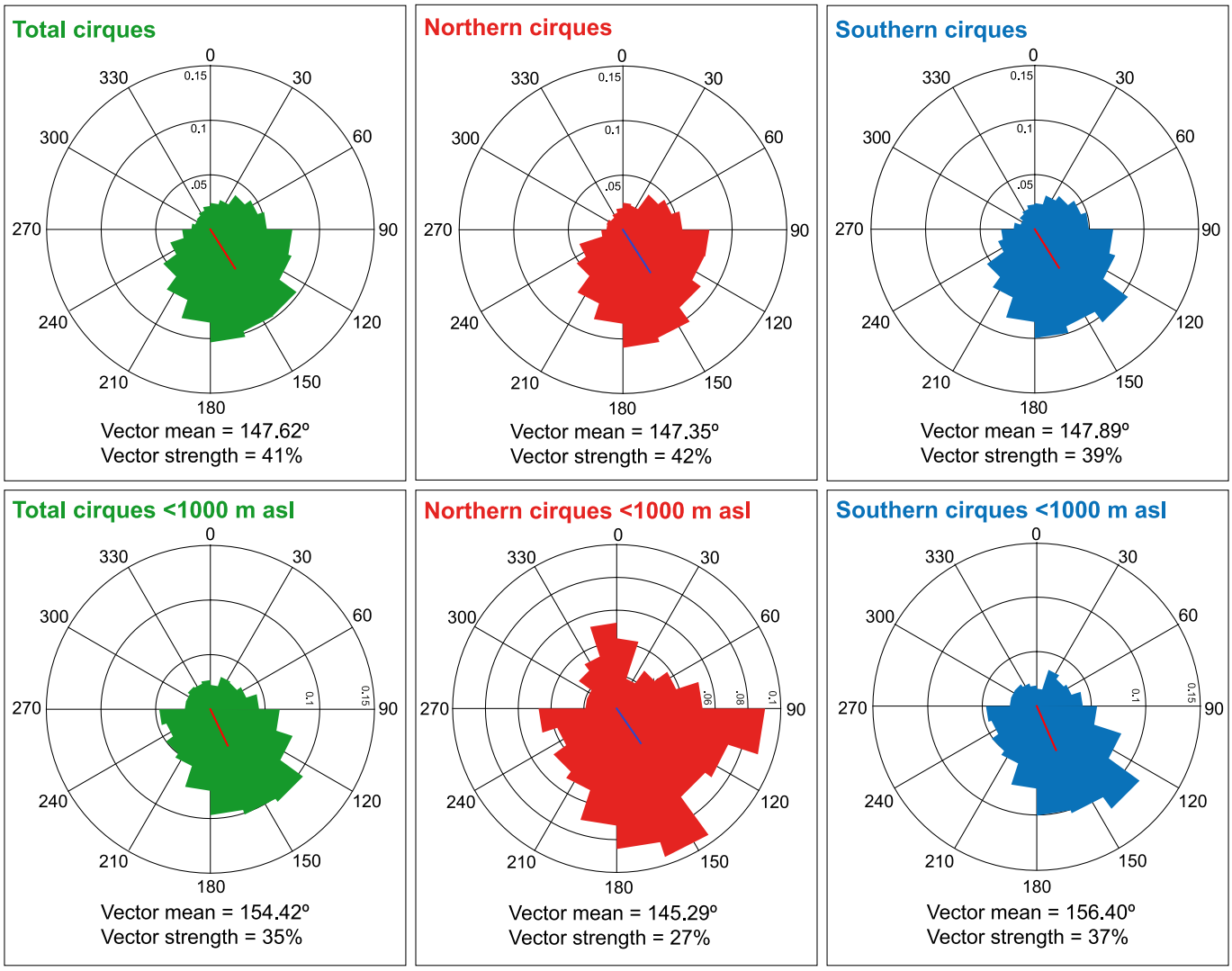

Fig. 7. Radial chart presenting cirque aspects in northern Patagonia. Line marks vector mean.

performed subsequent statistical analyses (i.e., PCA and one-way ANOVA) with mean annual climate parameters because correlations are stronger and thus we consider that they represent climate factors influencing the regional glacier mass balance.

The first two components of the PCA account for 78.76 % of the variance resulted from CFA and present-day climate variables along with geographic parameters influencing regional climate in the whole cirque population in northern Patagonia (Fig. 8). Component 1 indicates that longitude (Long) and distance to the coast (DTC) are strongly and positively correlated with CFA. Additionally, pure climate parameters such as total annual precipitation (Precip) and mean annual minimum temperature (Tmin) also exhibit a strong negative correlation with CFA. On the one hand, Component 1 incorporates the variables that better explain CFA distribution in northern Patagonia (51.11 % variance). On the other hand, component 2 suggests that latitude (Lat), incoming solar radiation (Rad) and mean annual maximum temperature (Tmax), in descending order of correlation, are a secondary contribution to CFA distribution in northern Patagonia (27.65 % variance).

4.5. *Regional geology, topography and cirque attributes in northern Patagonia*

Regional geological maps depict 23 bedrock units in northern Patagonia (Lizuaín and Panza, 2018; SERNAGEOMIN, 2003; Supplementary material). We grouped them in granitic (code 1), metamorphic (2), volcanic (3) and sedimentary (4) rock types. Most of the cirques in northern Patagonia are placed over granitoids (2228; 72.31 %), followed by volcanic (506; 16.42 %), metamorphic (227; 7.36 %) and sedimentary lithologies (120; 3.89 %).

The one-way ANOVA reveals that all cirque attributes exhibit *p*-values<0.05 indicating significant differences in cirque metrics between lithological classes, except for circularity (p-value $= 0.168$). However, width (p-value $= 0.341$) in the northern subpopulation and the L/W and circularity index (p-value $= 0.100$ and 0.076, respectively) in the southern subpopulation seem to present no significant differences with lithology classes (Table 6).

The longest (L) and widest (W) cirques of both populations are found in volcanic and sedimentary rocks, whereas the cirques presenting larger elevation ranges (H) are often carved onto metamorphic and sedimentary materials. The most circular (circularity and L/W) cirques in both subregions are predominantly volcanic in lithology followed by sedimentary and granitic. Incision metrics (L/H and W/H) tend to display greater values on volcanic materials, followed by metamorphic and granitic rocks in both subpopulations. Finally, the highest CFAs in the entire region are observed in volcanic rocks, followed by granitic and metamorphic lithologies (Supplementary material).

Our swath analysis of northern Patagonia reveals that cirques develop between the maximum (i.e., mostly stratovolcanoes edifices)

Table 4
Pearson correlation matrix between main geometry attributes of cirques in northern Patagonia and present-day climate variables (Fick and Hijmans, 2017). Correlations with * are statistically significant at $p < 0.05$. Bold values indicate correlations $r > 0.75$.

	L	W	L/W	L/H	W/H	Perim	Area_2D	Circularity	Lat	Long	DTC	Precip	Tmax	Tmin	Rad
L	**1.00**	**0.764***	0.407	0.367	0.004	**0.911***	**0.899***	−0.095	−0.166*	−0.076	−0.039	0.060	−0.001	0.088	−0.166*
W		**1.000**	−0.222	0.085	0.265	**0.932***	**0.908***	−0.012	−0.124*	−0.078	−0.102	0.053	0.109	0.178	−0.179*
L_W			**1.000**	0.413	−0.402	0.076	0.072	−0.048	−0.087	0.010	0.087	−0.071	−0.086	−0.032	−0.005
L_H				**1.000**	0.624*	0.218	0.227	−0.066	−0.048	0.043	0.189	−0.113	−0.064	−0.030	0.069
W_H					**1.000**	0.147	0.151	0.066	0.010	0.042	0.116	−0.072	−0.014	−0.017	0.067
Perimeter						**1.000**	**0.966***	0.095	−0.158*	−0.076	−0.074	0.079	0.017	0.096	−0.190*
Area_2D							**1.000**	0.010	−0.150*	−0.069	−0.071	0.074	0.030	0.098	−0.176*
Circularity								**1.000**	−0.084	0.009	−0.026	−0.048	−0.095	−0.035	−0.078
Lat									**1.000**	0.587*	0.558*	−0.283*	0.446	−0.315*	**0.875***
Long										**1.000**	**0.786***	**−0.886***	−0.112	**−0.766***	0.569*
DTC											**1.000**	**−0.746***	−0.092	−0.600*	0.599*
Precip												**1.000**	0.465*	**0.875***	−0.344*
Tmax													**1.000**	0.649*	0.479*
Tmin														**1.000**	−0.213*
Rad															**1.000**

Table 5
Pearson correlation matrix between altitudinal attributes (CFA) of cirques in northern Patagonia and present-day climate variables (Fick and Hijmans, 2017). Hypso corresponds to the hypsometric maximum, which is defined as the elevation bin that contains the largest surface area of the cirque. Correlations with * are statistically significant at $p < 0.05$. Bold values indicate correlations $r > 0.75$.

	CFA	Hmax	H	Hmean	Area_3D	Slope	Hypso	Lat	Long	DTC	Precip	Tmax	Tmin	Rad
CFA	**1.000**	**0.820***	−0.429*	**0.955***	−0.347*	−0.291*	**0.893***	0.528*	**0.838***	0.712*	**−0.839***	−0.357*	**−0.862***	0.479*
Hmax		**1.000**	0.166	**0.942***	0.105	0.042*	**0.893***	0.502*	**0.842***	0.660*	**−0.812***	−0.347*	**−0.865***	0.382*
H			**1.000**	−0.159*	**0.762***	0.568*	−0.130*	−0.112*	−0.112*	−0.185*	0.164*	0.067	0.121	−0.221*
H_Mean				**1.000**	−0.154*	−0.132*	**0.956***	0.543*	**0.880***	0.724*	**−0.868***	−0.373*	**−0.908***	0.458*
Area_3D					**1.000**	0.137*	−0.148*	−0.145*	−0.085*	−0.010*	0.104	0.050	0.116	−0.191*
Slope						**1.000**	−0.085*	0.009*	−0.142*	−0.287*	0.250*	0.152	0.144	−0.148*
Hypso							**1.000**	0.514*	**0.834***	0.681*	**−0.826***	−0.361*	**−0.868**	0.434*
Lat								**1.000**	0.587*	0.558*	−0.283*	0.446	−0.315*	**0.875***
Long									**1.000**	**0.786***	**−0.886***	−0.112*	**−0.766***	0.569*
DTC										**1.000**	−0.746*	−0.085*	−0.591*	0.594*
Precip											**1.000**	0.465*	**0.875***	−0.344*
Tmax												**1.000**	0.649*	0.479*
Tmin													**1.000**	−0.213*
Rad														**1.000**

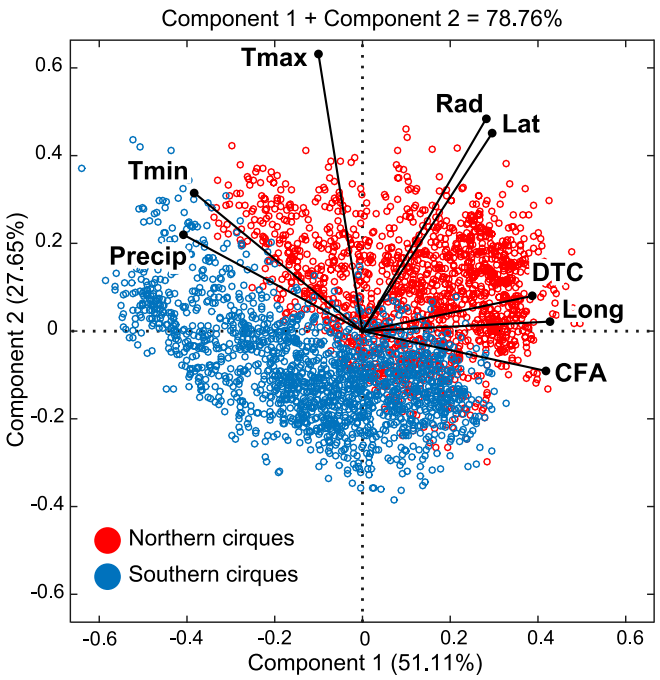

Fig. 8. PCA of potential controls on altitudinal distribution of cirques (CFA) in northern Patagonia. The blue and red dots depict the northern and southern cirques, respectively. (For interpretation of the references to colour in this figure legend, the reader is referred to the web version of this article.)

and mean topography (i.e., mostly non-volcanic ranges) of the region from <100 to ~2000 m asl (Fig. 9). On the one hand, following a west-to-east axis, the northern cirques are exclusively located in the Cordillera de los Andes between ~72.7° and ~ 71.2° W. CFA of this subpopulation rises in altitude eastwards from <500 to <2000 m asl. CFA rising trend is gentler than those of the mean topography and it decouples from it and begins to gain elevation towards the maximum altitudes at ~71.8° W. On the other hand, the southern subpopulation extends between ~74.6° and ~ 71.2° W comprising the Pacific archipelagos and the Patagonian Andes. CFA tends to maintain a relatively constant elevation between <100 and ~ 1000 m asl across the Pacific islands and the main range foothills and then rapidly increases in elevation following the western mountain flank until ~2000 m asl. Similar to the northern cirques, the initial increase in elevation is parallel with the rise in mean topography until ~71.8° W when the mean elevation tends to stabilize at ~1000 m asl while CFA continues increasing more or less linearly towards maximum elevations (Fig. 9).

5. Discussion

5.1. Controlling factors of cirque morphometry and distribution in northern Patagonia

Cirques are glacial landforms, therefore, it is widely assumed that climate factors such as temperature, precipitation and incoming solar radiation along with modulating geographic parameters, such as latitude/longitude and distance from moisture sources, exert a strong control on cirque morphometry and distribution (Barr and Spagnolo, 2015a). Furthermore, the influence of bedrock lithology and local topography on cirque characteristics have also been widely demonstrated in prior studies (e.g., Hughes et al., 2007; Delmas et al., 2014; Crest et al., 2017).

5.1.1. Climatic controlling factors

Assuming that northern Patagonia exhibits similar climate patterns at present to those in the past but with differences in magnitude, high statistical correlations indicate that the altitudinal distribution of cirques, equating to the CFA, is mainly linked to the spatial behavior of mean annual minimum temperatures ($r > -0.86$) and annual total precipitation ($r > -0.84$). Precipitation and temperatures are both west-to-east zonal expressions of the impact of the SWW. The strong correlation between CFA and longitude ($r > 0.84$) and distance to coast (DTC; $r > 0.71$) point to the westerly atmospheric circulation as a major controlling factor for CFA distribution. While correlations between climate parameters are virtually indistinguishable, precipitation exhibits a stronger correlation with longitude and DTC than temperatures (Table 4). Although cooling is crucial for glaciers to grow, zonally, the importance of precipitation with longitude is well represented by the linear upward trend of CFA progressively inland, enhanced by the orographic effect (Fig. 6b and Fig. 9). Moreover, although minimum temperatures decrease inland due to Andean high elevations and continentality, CFA trend continues to rise eastwards (Fig. 2b and Fig. 9). Considering that both precipitation and temperatures are partially modulated by altitude, we infer that total annual precipitation (i.e., snowfall) is most likely the main controlling factor governing CFA distribution from west to east. Outside Patagonia, available studies have documented similar correlations between CFA and DTC in areas under strong maritime influence, such as Scandinavian Peninsula (Oien et al., 2022), Iceland (Ipsen et al., 2018; Principato and Lee, 2014), Faroe Islands (Wallick and Principato, 2020) and Kamchatka Peninsula (Barr and Spagnolo, 2015a).

Additionally, moderate correlation between CFA and solar radiation ($r > 0.48$) suggests a weaker role of the radiative balance in cirque altitudinal distribution. Nevertheless, strong correlation between radiation and latitude ($r > 0.87$; Table 4) indicates that the radiation balance exerts control on the distribution of cirques to some extent, which is observable in the steady poleward lowering of CFA. However, incident radiation is also impacted by altitude, obscuring direct correlations with CFA. The observed tendency of northern Patagonian cirques is consistent with worldwide assessment of cirque aspects determining that poleward orientations are linked in a major way to solar radiation

Table 6
One-way ANOVA of main geometry attributes of cirques and regional geology classes. All variables are deemed statistically significant when p-value<0.05.

	All cirques		Northern sector cirques		Southern sector cirques	
	F	P-Value	F	P-Value	F	P-Value
L	5.755	<0.001	2.984	0.030	4.489	0.004
W	3.622	0.013	1.116	0.341	3.921	0.008
H	7.215	<0.001	3.663	0.012	7.391	<0.001
CFA	144.018	<0.001	43.479	<0.001	107.841	<0.001
L/W	3.394	0.017	5.110	0.002	2.087	0.100
L/H	38.359	<0.001	22.679	<0.001	16.935	<0.001
W/H	27.002	<0.001	9.882	<0.001	16.031	<0.001
Circularity	1.686	0.168	2.871	0.035	2.293	0.076

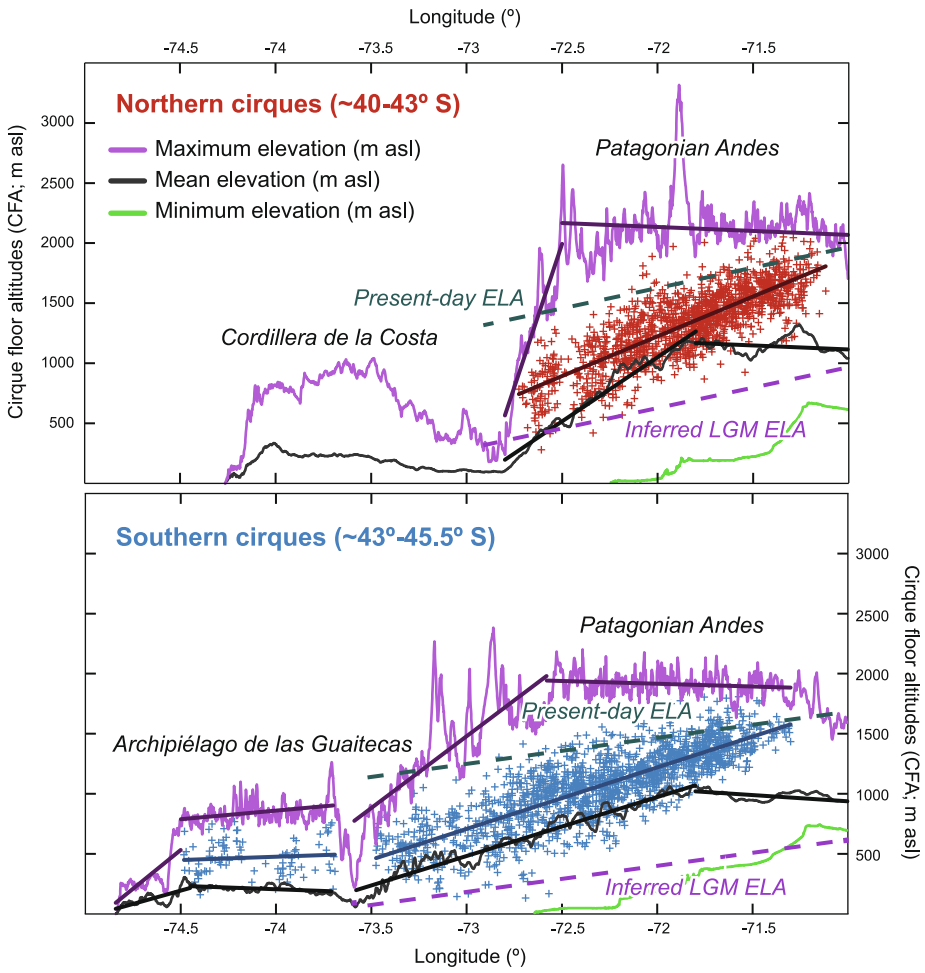

Fig. 9. Swath profile of the topography between a) ~40°-43° S and b) ~43°-45.5° S across northern Patagonia. Red and blue crosses depict the northern and southern cirque subpopulations, respectively. For comparison to CFAs, present-day ELAs are inferred from Carrivick et al. (2016) and the Chilean Glacier Inventory (DGA, 2022), while LGM ELAs are based on Denton et al. (1999a, 1999b) and Yan et al. (2022). (For interpretation of the references to colour in this figure legend, the reader is referred to the web version of this article.)

receipt (Evans, 2006b).

Furthermore, the dominant SE-SSE cirque orientation (vector mean = 147.62°) is most likely resulting from the effects of both solar radiation receipt and the influence of the SWW. First, incoming solar radiation regulates cirque aspects through the so-called "morning-afternoon effect" (Evans, 1977) by which, in the southern hemisphere, east-to-south slopes receive most solar radiation during the morning, when temperatures are lower and, thus, snow and ice tend to persist for longer intervals facilitating glacier growth. Given that the vector strength of cirque orientations is moderate (~41 %), we infer that radiation receipt derived from the "morning-afternoon effect" could act as a complementary controlling factor. Second, cirques aspects are also likely reflecting snow drifting to lee slopes promoted by prevailing westerly circulation. In general, we infer that relatively weak correlations between CFA, aspects and radiation suggest that westerly-driven precipitation might be an important controlling factor, as well. Our interpretation is consistent with available analyses concluding that although solar radiation receipt plays a significant role, wind-effect might be an additional key factor on cirque development, particularly in moderate relief areas (Evans, 2006b; Pedraza et al., 2019).

Finally, the observed correlation between CFA and climate parameters seems to be in line with studies of ELA sensitivity experiments conducted on present-day Andean glaciers (Sagredo et al., 2014), which suggest that the distribution of cirques is consistent with the pattern exhibited by contemporary mass balance gradients (Carrasco-Escaff et al., 2023) and, thus, we infer that similar controlling factors influenced the distribution of mountain glaciers during past glacial intervals.

5.1.2. *Non-climatic controlling factors*

The One-way ANOVA analysis indicates significant morphometric disparities between cirques in each bedrock type (Table 6 and Fig. 9). Hence, we interpret that local lithology regulates to some extent cirque morphometry and CFA in northern Patagonia. Additionally, weak correlations between present-day climate variables and cirque dimensions (Table 3) might be reflecting that processes depending on non-climate factors are governing cirque geometrical development, such as regional lithologies' erodibility. However, we argue that bedrock types play a secondary role in CFA distribution because, at this latitude, both the Andes and associated lithologies run with a north-south trend. Therefore, the changes in regional lithological units also match the zonal topography gradient and, consequently, elevation above sea level. Accordingly, from west to east, lowest cirques are often hosted in metamorphic rocks forming the Pacific archipelago and highest cirques are often in areas dominated by granitic rocks of the Patagonian Andes (Supplementary material). This is also supported by the one-way ANOVA showing significant differences between CFA and rock types in northern Patagonia.

Regional topography is also expected to be a major non-climatic modulator on CFA distribution. However, in the northernmost cirques, the eastward CFA increasing tendency broadly matches the gradient of

the mean topography and is totally decoupled from it east of 71.8° W (Fig. 9). Moreover, it is worth noting that the mean elevation of the Patagonian Andes increases very rapidly in its western flank before reaching constant elevations of ~1000 m asl, whereas the cirques exhibit a relative linear rising towards the interior of the continent reaching ~1500 m asl (Fig. 9). The southern population of cirques can be divided in two groups, cirques located in Archipiélago de las Guaitecas and cirques in the Patagonian Andes. The first group exhibits a relative homogeneous elevation following the tendency of the highest topography. Conversely, cirques in the Andes rise closely parallel to the gradient of the mean topography until they continue gaining elevation whereas the mean topography starts to decrease at 71.8° W. In northern Patagonia, a strong orographic effect has been reported (Garreaud et al., 2013), presenting an eastward progressive declining tendency of precipitation while Andean topography increases. Considering the behavior of cirques and topography described above, and the strong statistical correlations between CFA, precipitation and DTC, we posit that topography is a subsidiary controlling factor to explain cirque distribution in northern Patagonia. Our interpretation is in line with several studies conducted in maritime environments that concluded that inland increasing elevations are most likely promoting moisture starvation and, consequently, cirques respond to a coupled effect of precipitation and topography (Barr et al., 2017; Barr and Spagnolo, 2015a; Oien et al., 2022; Wallick and Principato, 2020).

Additionally, topography controls the so-called glaciation threshold, which corresponds to the amount of land above ELAs suitable for glacier development (Porter, 1977, 1989). In northern Patagonia, most of the cirques are emplaced well below the highest summits (Fig. 9) and, thus, suitable areas for glaciers to grow are not a limiting factor in the region. We propose that if cirques are not located at maximum elevations, then it is because either the highest topographic emplacements were frequently covered by an ice sheet, preventing cirque formation during full glacial conditions or because prevailing interglacial climate conditions were not favorable for cirque development. This implies that cirques would have been active exclusively during short periods before and after the existence of an ice sheet. Therefore, we infer that regional altitudinal variability (i.e., topography) serves as a complement to local glacial history (i.e., development of large ice bodies) as a controlling factor of cirque distribution. Our inferences are in line with the model proposed by Oien et al. (2022), in which topo-climatic gradients along with local cryosphere evolution explain spatial distribution of cirques in the Scandinavian Peninsula.

5.2. *Palaeoglacial and palaeoclimate inferences based on cirque morphometry and spatial distribution*

Cirques are considered robust indicators of palaeoglacial and palaeoclimate conditions. Generally, the circularity indices, aspect symmetry and CFA have been interpreted as reflecting the typology of glaciers during past glaciations and the intensity of glacial erosion processes (Křížek and Mida, 2013). In addition, CFA is also considered a suitable proxy for ELA when glaciers were constrained to the cirque (e.g., Ipsen et al., 2018; Principato and Lee, 2014). Finally, cirque aspects have been used to infer prevailing wind directions (e.g., Pedraza et al., 2019; Zhang et al., 2021; Li et al., 2023).

5.2.1. *Palaeoglacial inferences*

In northern Patagonia, naturally circular cirques are ubiquitous as revealed by plan form index (circularity = 1.06 ± 0.37), whereas the elongation ratio indicates that length and width often present the same dimensions (L/W = 0.99 ± 0.26). Especially north of ~43° S, isometry/allometry analysis (i.e., size) shows a remarkedly high vertical growth of cirques (exponent H = 1.04), matching or outpacing lengthening and widening. Globally, most cirque studies have reported H exponents to be lower than L and W exponents, except for New Zealand (exponent H = 1.01; Brook et al., 2006; Barr and Spagnolo, 2015b) and the central Himalayas (exponent H = 1.11; Li et al., 2023). Consequently, to our knowledge, the exponent H for Patagonian northernmost cirques is likely one of the highest ever documented worldwide (Barr and Spagnolo, 2015b). Such intense vertical development might be denoting the long-term presence of small glaciers, which would enhance localized subglacial erosion within cirques promoting their deepening. Outside Patagonia, studies have detected relatively isometric cirques in the Southern Alps of New Zealand (Brook et al., 2006), the French Pyrenees (Delmas et al., 2014), Kamchatka Peninsula (Barr and Spagnolo, 2013) and the Tibetan Plateau (Zhang et al., 2021).

Prior studies have concluded that cirque isometry/allometry analysis might be a suitable proxy for glacial processes only when the local rocks are sufficiently isotropic for responding to cold conditions homogeneously and if independent evidence exists indicating that cirques are climate-formed (Delmas et al., 2015). Given that the majority of cirques in northern Patagonia are hosted in isotropic granitic lithologies (Pankhurst et al., 1999; >70 % of cirques; Supplementary material) and that intense glacial activity in the region started as early as the Miocene (Mercer and Sutter, 1982; Herman and Brandon, 2015; Willett et al., 2020), we hypothesize that erosional processes linked to long-lasting cirque-type glaciers dominated the northern Patagonian Andes in the past. Our interpretation is also supported by one-way ANOVA indicating that circular cirques are common in all bedrock types in the region.

In addition, cirque aspects also yield insights into glaciation magnitude according to the "Law of decreasing glacial asymmetry with increasing glacier cover" (Evans, 1977). The latter proposes that during less-extensive glaciations with moderate ELA depression, glaciers will mostly grow on favorable-oriented slopes, resulting in asymmetric cirque aspects that represent these optimal slopes. According to Evans (1977), cirques in northern Patagonia are markedly asymmetric (41 %). Worldwide, mid-latitude regions formerly covered by relatively extensive ice sheets, such as the Asian mountain ranges, the Scandinavian Peninsula and the Kamchatka Peninsula, exhibit cirque aspects ranging between 8 and 46 % vector strength (Barr et al., 2024). Therefore, we interpret that the vector strength of our cirque population represents relatively high asymmetry compared to regions with similar glacial histories. Consequently, we argue that widespread SSE-SE cirques further support our hypothesis of predominant cirque-type glaciations in northern Patagonia, particularly outside globally coldest glacial maxima.

Furthermore, low-elevation cirques have been interpreted as reflecting intense cooling events linked to glacial maxima because major ELA depressions are required for these cirques to host active glaciers (Oien et al., 2022; Li et al., 2023). In northern Patagonia, particularly north of 43°, the cirques located below 1000 m asl exhibit a remarkable reduction in aspect asymmetry (to a strength of 27 %), suggesting that these cirques were likely active during episodes of extensive ice cover (Fig. 7). Additionally, lower cirques tend to be larger in area and display less-circular plan forms, which may be the result of enhanced glacial erosion (Fig. 10). Given that low-elevation cirques in northern Patagonia are a minority (n = 898; ~29 %; Supplementary material) and were most likely active during short intervals of ice sheet grow and decay, we conclude that cirque-type glaciers have been particularly common in the region during past glacial-interglacial cycles.

Overall, we posit that northern Patagonia hosted less-extensive glaciations more often than the southernmost region because the former corresponds to the northernmost limit of past ice sheets during past glaciations, so it likely exhibited suboptimal climate conditions for glaciers to grow extensively. Furthermore, glacial chronologies and modelling experiments in the region have shown that large ice sheets tended to disintegrate very rapidly after glacial maxima forming small glaciers and ice caps near the highest Andean headwalls (Cuzzone et al., 2024; Leger et al., 2021; Moreno et al., 2021, 2022; Soteres et al., 2022a, 2022b). Therefore, we infer that small glaciers and ice caps were common in northern Patagonia during past glacial-interglacial cycles, especially outside glacial maxima stricto sensu (i.e., often within

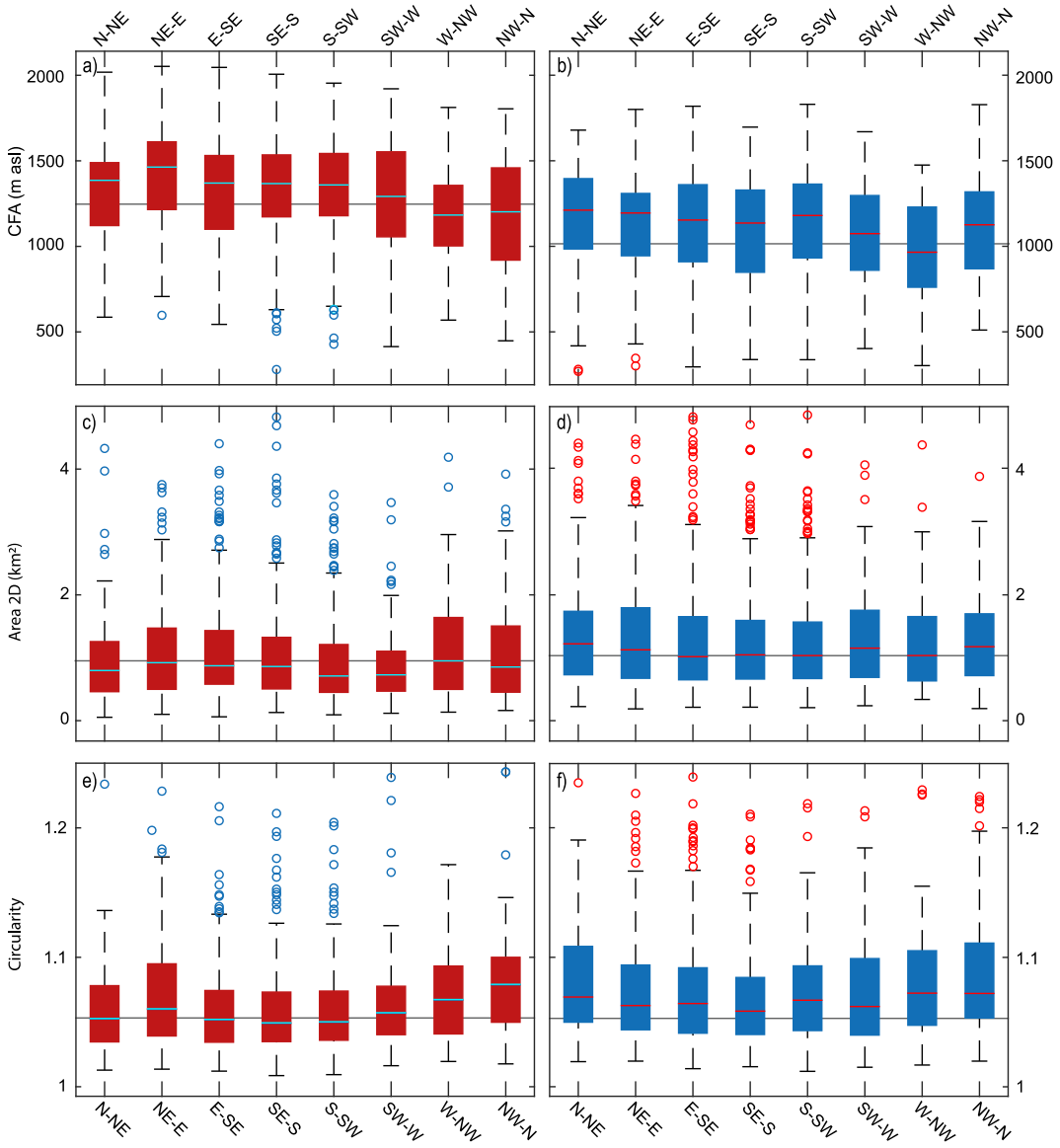

Fig. 10. Boxplots of cirque metrics against aspects in the northern (red) and southern (blue) cirque subpopulation in northern Patagonia. a) and b) CFA; c) and d) Area; e) and f) Circularity. Grey lines are the mean value of each attribute per cirque subpopulation. (For interpretation of the references to colour in this figure legend, the reader is referred to the web version of this article.)

interglacial marine isotope stages, such as MIS 3 and MIS 5).

5.2.2. *Palaeoclimate inferences*

Both direct and indirect estimates averages of modern ELA in northern Patagonia broadly show a poleward decrease from ~2000 to ~1400 m asl between ~40° and ~ 45° S of latitude, and an inland rise from ~1300 to ~1600 m asl between ~71.5° and ~ 74.5° W of longitude (Bravo et al., 2021; Carrivick et al., 2016; DGA, 2022; Falaschi et al., 2019; Sagredo et al., 2017; Schaefer et al., 2020). Our first-order cirques ELA elevations indicate a steady poleward decline of CFA ranging between ~700 and ~ 400 m and inland rise ranging between ~500 and ~ 300 m below the modern ELA (Fig. 9 and Fig. 10). We acknowledge that averaging ELAs over ~5° in latitude generates considerable uncertainties. However, we infer that this error does not affect our interpretations, given that the number of CFA anomalies regarding the ELA is negligible (i.e., ~50 cirques or ~ 2 % of the total population). Therefore, considering that empirical evidence and numerical modelling estimated an average ~ 1200–1000 m drop of the regional ELA during the LGM (Hulton et al., 1994; Denton et al., 1999b; Sugden et al., 2002; Hubbard et al., 2005; Peltier et al., 2021; Yan et al., 2022), we argue that our averaged cirque-based ELA estimation is likely reflecting intermediate glacial-interglacial palaeoclimate.

CFAs lie in general between Holocene and LGM elevations (Fig. 9). Recent modelling experiments supported by highly-resolved glacial chronologies in northern Patagonia reveal repeated glacier fluctuations coeval with millennial-scale cold snaps detected in Antarctic ice cores during T1 (Moreno et al., 2022; Soteres et al., 2022b). Overall, cirque-based palaeo-ELAs broadly match with ELA reconstructions for these cold excursions which encompassed ~2–3 °C drop on temperatures along with a 20–50 % increase of precipitation relative to the present (Leger et al., 2021; Muir et al., 2023; Sagredo et al., 2018), which is less than half of the coldest glacial maxima estimations of ~6-8° C (Denton et al., 1999b; Cuzzone et al., 2024). Additional studies in Patagonia also show glaciers fluctuating and thus cold conditions throughout much of MIS 3 (e.g., García et al., 2018). This climate variability prior to the coldest LGM likely encompassed multiple intervals of T1-like climate. Accordingly, we hypothesize that cirques reach their maximum activity within periods occurring either at the beginning and/or the ending of a

full glacial-cold intervals. If correct, cirque-derived ELAs in this study are most likely representative of intermediate climate conditions at least throughout the late Quaternary Period matching "average conditions" of Porter (1989) or "longest-lasting conditions" of Spagnolo et al. (2022).

5.3. Comparison of morphometric attributes and altitudinal distribution across Patagonian cirques

The Sierra Baguales range (~50°-51° S; Araos et al., 2018) is a peripheral mountain range in southern Patagonia located outside the inferred limits of the PIS, at least during the LGM (Davies et al., 2020). Local cirques (n = 143) are smaller than those in northern Patagonia with a mean circularity index and L/W of 1.065 and 0.91, respectively. Given that the glacial history of Sierra Baguales differs from northern Patagonia, it is not a suitable location for direct palaeoglacial comparisons. Nevertheless, circularity and elongation attributes suggest a dominance of circular cirques, potentially reflecting the prevalence of cirque-type glaciers. However, in Sierra Baguales almost one third of the population exhibits elongated plan forms often connected to U-shaped valleys with moraine ridges (Davies et al., 2020). The heterogeneity of cirque shape parameters in Sierra Baguales points to a complex evolution but it is likely that cirque-type glaciers were common in Sierra Baguales because valley glaciers occurred only during extreme glacial conditions.

Farther south, cirques (n = 251 cirques) of Tierra del Fuego (~54.4° S; Oliva et al., 2020) are also smaller than those in northern Patagonia but present a slightly higher mean circularity of 1.10 and L/W ratio of 1.08, which implies erosional processes associated with ice flowing out of the cirques. In addition, isometry/allometry analysis indicates that lengthening and widening outpaced deepening in half of the studied population, supporting significant valley glacier activity (Oliva et al., 2020). Available glacial chronologies suggest that after the initial PIS withdrawal from the Fueguian Andes during T1, small glaciers near their cirques fluctuated following an Antarctic style (Hall et al., 2019; Hall et al., 2013; Menounos et al., 2013). Overall, the glacial history of these cirques appears analogous to that in northern Patagonia during past glaciations. Based on our results, we hypothesize that the disparities in cirque geometric attributes between northern and southern Patagonia may reflect different rates of glacier development due to the latitudinal climate gradient. Consequently, longer climate intervals favoring extensive glaciers prevailed in Tierra del Fuego, leading to a rapid transition from cirque-type to valley glacier and thereby preventing prolonged periods of cirque enlargement and deepening. Overall, this implies that glaciers in southern Patagonia might have grown into an ice sheet more frequently than their counterparts in northern Patagonia.

In general, CFA and dominant aspects of cirques in southern Patagonia are consistent with a strong control of westerly circulation and incoming solar radiation variations (Araos et al., 2018; Oliva et al., 2020). Therefore, the morphometry and spatial distribution of cirques across the whole Patagonian region was climatically driven with limited influence of non-climate factors, such as local geology and topography.

6. Conclusions

We examine the morphometric attributes of a large population of cirques (n = 3081) for the first time in Patagonia, producing a geomorphic database unprecedented for such landforms in South America. Systematic mapping along with statistical analysis of cirques metrics, present-day climate parameters and regional geology allow us to test the suitability of cirques as proxies of former glacial and climate conditions for the Andes. We conclude that cirque geometrical characteristics can be influenced by geological factors, although climate plays a significant role as well. Moreover, as geologic patterns can be similar to climatic trends from west to east, they may work hand-in-hand to influence cirque geometries. Climate variables linked to the behavior of the Southern Westerly Winds, especially annual total precipitation, mainly govern cirque spatial arrangements, particularly altitudinal distribution and aspects. However, the relative importance of these climate factors may vary spatially. Based on statistical correlations between cirque geometry attributes, altitudinal distribution and present-day climate variables, we conclude that cirque-type glaciers and small ice caps were the most frequent cryospheric state in northern Patagonia during the Quaternary (cf., southernmost Patagonia-Fuego). We conclude that during much of the Quaternary Period, northern Patagonia cirques contained active glaciers independent of the ice sheet, likely because the locus of the Southern Westerly Winds tends to be relatively poleward (e.g., in summer), especially outside full-glacial maximum positions. The SWW represents a major climate boundary with colder air to the south (e.g., Garreaud et al., 2013), in addition to the effect on precipitation patterns. This situation (cf., "average conditions" of Porter (1989)) promotes less extensive glaciations with no large ice sheet development at least north of ~45°S, during much of a glacial cycle. Our study reveals the value of cirques as indicators of palaeoglacial and palaeoclimate evolution including over different timescales, and thus, encourages further research in Patagonia and other mountain ranges of the Southern Hemisphere.

CRediT authorship contribution statement

R.L. Soteres: Writing – review & editing, Writing – original draft, Investigation, Funding acquisition, Formal analysis, Data curation, Conceptualization. **D.A. Cabrera:** Investigation, Formal analysis, Data curation. **M.A. Martini:** Writing – review & editing, Investigation, Formal analysis, Data curation. **E.A. Sagredo:** Writing – review & editing, Investigation, Funding acquisition. **J. Pedraza:** Writing – review & editing, Investigation, Conceptualization. **R.M. Carrasco:** Writing – review & editing, Investigation, Funding acquisition, Conceptualization. **M.R. Kaplan:** Writing – review & editing, Investigation, Conceptualization. **J.M. Araos:** Writing – review & editing, Investigation.

Declaration of competing interest

The authors declare that they have no known competing financial interests or personal relationships that could have appeared to influence the work reported in this paper.

Acknowledgements

This research was framed and funded by the ANID FONDECYT postdoctoral grant #3220537, the ANID BASAL CHIC #FB210018 and the ANID FONDECYT Regular #1220550. It is also part of the project reference PID2020-117685GB-I00 funded by MCIU/AEI/ 10.13039/501100011033 and the project funded by the grant reference 2022-GRIN-34112 and the European Regional Development Fund (ERDF). MK acknowledges support by National Science Foundation NSF EAR-1804816. The authors are grateful to Dr. Ian S. Evans and an anonymous reviewer for their insightful comments that contributed to improving this article.

Appendix A. Supplementary data

Supplementary data to this article can be found online at https://doi.org/10.1016/j.palaeo.2025.112939.

Data availability

Raw data extracted from digital elevation models and gridded present-day climate parameters used in this study are freely available as Supplementary Material.

References

Anders, A.M., Mitchell, S.G., Tomkin, J.H., 2010. Cirques, peaks, and precipitation patterns in the Swiss Alps: Connections among climate, glacial erosion, and topography. Geology 38 (3), 239–242. https://doi.org/10.1130/G30691.1.

Andersen, B.G., Denton, G.H., Lowell, T.V., 1999. Glacial geomorphologic maps of Llanquihue drift in the area of the southern Lake District, Chile. Geogr. Ann. Ser. B 81A (2), 155–166. https://doi.org/10.1111/1468-0459.00056.

Araos, J.M., Le Roux, J.P., Kaplan, M.R., Spagnolo, M., 2018. Factors controlling alpine glaciations in the sierra baguales mountain range of southern Patagonia (50° s), inferred from the morphometric analysis of glacial cirques. Andean Geology 45 (3), 357–378. https://doi.org/10.5027/andgeoV45n3-2974.

Barr, I.D., Spagnolo, M., 2013. Palaeoglacial and palaeoclimatic conditions in the NW Pacific, as revealed by a morphometric analysis of cirques upon the Kamchatka Peninsula. Geomorphology 192, 15–29. https://doi.org/10.1016/j.geomorph.2013.03.011.

Barr, I.D., Spagnolo, M., 2015a. Understanding controls on cirque floor altitudes: Insights from Kamchatka. Geomorphology 248, 1–13. https://doi.org/10.1016/j.geomorph.2015.07.004.

Barr, I.D., Spagnolo, M., 2015b. Glacial cirques as palaeoenvironmental indicators: their potential and limitations. Earth-Science Reviews 151, 48–78. https://doi.org/10.1016/j.earscirev.2015.10.004.

Barr, I.D., Ely, J.C., Spagnolo, M., Clark, C.D., Evans, I.S., Pellicer, X.M., Pellitero, R., Rea, B.R., 2017. Climate patterns during former periods of mountain glaciation in Britain and Ireland: Inferences from the cirque record. Palaeogeography, Palaeoclimatology, Palaeoecology 485, 466–475. https://doi.org/10.1016/j.palaeo.2017.07.001.

Barr, I.D., Ely, J.C., Spagnolo, M., Evans, I.S., Tomkins, M.D., 2019. The dynamics of mountain erosion: Cirque growth slows as landscapes age. Earth Surf. Process. Landf. 44 (13), 2628–2637. https://doi.org/10.1002/esp.4688.

Barr, I.D., Spagnolo, M., Rea, B.R., Bingham, R.G., Oien, R.P., Adamson, K., Ely, J.C., Mullan, D.J., Pellitero, R., Tomkins, M.D., 2022. 60 million years of glaciation in the Transantarctic Mountains. Nature Communications 13 (1). https://doi.org/10.1038/s41467-022-33310-z.

Barr, I.D., Spagnolo, M., Tomkins, M.D., 2024. Cirques in the transantarctic mountains reveal controls on glacier formation and landscape evolution. Geomorphology 445, 108970. https://doi.org/10.1016/j.geomorph.2023.108970.

Bathrellos, G.D., Skilodimou, H.D., Maroukian, H., 2014. The spatial distribution of middle and late pleistocene cirques in Greece. Geogr. Ann. Ser. B 96 (3), 323–338. https://doi.org/10.1111/geoa.12044.

Benn, D.I., Lehmkuhl, F., 2000. Mass balance and equilibrium-line altitudes of glaciers in high-mountain environments. Quat. Int. 65–66, 15–29. https://doi.org/10.1016/S1040-6182(99)00034-8.

Berens, P., 2009. CircStat: a MATLAB toolbox for circular statistics. J. Stat. Softw. 31 (10), 1–21. https://doi.org/10.18637/jss.v031.i10.

Bravo, C., Bozkurt, D., Ross, A.N., Quincey, D.J., 2021. Projected increases in surface melt and ice loss for the Northern and Southern Patagonian Icefields. Sci. Rep. 11 (1), 1–13. https://doi.org/10.1038/s41598-021-95725-w.

Brook, M.S., Kirkbride, M.P., Brock, B.W., 2006. Cirque development in a steadily uplifting range: rates of erosion and long-term morphometric change in alpine cirques in the Ben Ohau Range, New Zealand. Earth Surf. Process. Landf. 31, 1167–1175. https://doi.org/10.1002/esp.

Brown, R.M., 1905. Cirques: A review. Bull. Am. Geogr. Soc. 37 (2), 86–91.

Caldenius, C.C., 1932. Las glaciaciones cuaternarias en la Patagonia y Tierra del Fuego. Geogr. Ann. Ser. B 14, 1–164.

Caro, A., Condom, T., Rabatel, A., 2021. Climatic and morphometric explanatory variables of glacier changes in the Andes (8–55°S): new insights from machine learning approaches. Front. Earth Sci. 9 (December), 1–21. https://doi.org/10.3389/feart.2021.713011.

Carrasco-Escaff, T., Rojas, M., Garreaud, R.D., Bozkurt, D., Schaefer, M., 2023. Climatic control of the surface mass balance of the Patagonian Icefields. The Cryosphere 17 (3), 1127–1149. https://doi.org/10.5194/tc-17-1127-2023.

Carrivick, J.L., Davies, B.J., James, W.H.M., Quincey, D.J., Glasser, N.F., 2016. Distributed ice thickness and glacier volume in southern South America. Global Planet. Change 146, 122–132. https://doi.org/10.1016/j.gloplacha.2016.09.010.

Cembrano, J., Hervé, F., Lavenu, A., 1996. The Liquiñe Ofqui fault zone: a long-lived intra-arc fault system in southern Chile. Tectonophysics 259, 55–66. https://doi.org/10.1016/0040-1951(95)00066-6.

Clague, J.J., Barendregt, R.W., Menounos, B., Roberts, N.J., Rabassa, J., Martinez, O., Ercolano, B., Corbella, H., Hemming, S.R., 2020. Pliocene and Early Pleistocene glaciation and landscape evolution on the Patagonian Steppe, Santa Cruz province, Argentina. Quaternary Science Reviews 227, 105992. https://doi.org/10.1016/j.quascirev.2019.105992.

Cooper, E.L., Thorndycraft, V.R., Davies, B.J., Palmer, A.P., García, J.L., 2021. Glacial geomorphology of the former Patagonian Ice Sheet (44–46 °S). J. Maps 17 (2), 802–822. https://doi.org/10.1080/17445647.2021.1986158.

Crest, Y., Delmas, M., Braucher, R., Gunnell, Y., Calvet, M., 2017. Cirques have growth spurts during deglacial and interglacial periods: evidence from 10Be and 26Al nuclide inventories in the central and eastern Pyrenees. Geomorphology 278, 60–77. https://doi.org/10.1016/j.geomorph.2016.10.035.

Cuzzone, J., Romero, M., Marcott, S.A., 2024. Modeling the timing of Patagonian Ice Sheet retreat in the Chilean Lake District from 22-10 ka. Cryosphere 18 (3), 1381–1398. https://doi.org/10.5194/tc-18-1381-2024.

Davies, B.J., Darvill, C.M., Lovell, H., Bendle, J.M., Dowdeswell, J.A., Fabel, D., García, J.L., Geiger, A., Glasser, N.F., Gheorghiu, D.M., Harrison, S., Hein, A.S., Kaplan, M.R., Martin, J.R.V., Mendelová, M., Palmer, A., Pelto, M., Rodés, A., Sagredo, E.A., Thorndycraft, V.R., 2020. The evolution of the Patagonian Ice Sheet from 35 ka to the present day (PATICE). Earth Sci. Rev. https://doi.org/10.1016/j.meegid.2020.104171.

de Charpentier, J., 1823. Essai sur la constitution géognostique des Pyrénées. F-G Levrault.

Delmas, M., Gunnell, Y., Calvet, M., 2014. Environmental controls on alpine cirque size. Geomorphology 206, 318–329. https://doi.org/10.1016/j.geomorph.2013.09.037.

Delmas, M., Gunnell, Y., Calvet, M., 2015. A critical appraisal of allometric growth among alpine cirques based on multivariate statistics and spatial analysis. Geomorphology 228, 637–652. https://doi.org/10.1016/j.geomorph.2014.10.021.

Denton, G.H., Heusser, C.J., Lowell, T.V., Moreno, P.I., Andersen, B.G., Heusser, L.E., Schluchter, C., Marchant, D.R., 1999a. Interhemispheric Linkage of Paleoclimate druing the last Glaciation. Geogr. Ann. Ser. B 81 (2), 107. https://doi.org/10.1111/j.0435-3676.1999.00055.x.

Denton, G.H., Lowell, T.V., Heusser, C.J., Schlüchter, C., Andersen, B.G., Heusser, L.E., Moreno, P.I., Marchant, D.R., 1999b. Geomorphology, stratigraphy, and radiocarbon chronology of Llanquihue drift in the area of the southern Lake District, Sena Reloncaví, and Isla Grande de Chiloé, Chile. Geogr. Ann. Ser. B 81A (2), 167–229. https://doi.org/10.1111/1468-0459.00057.

Denton, G.H., Anderson, R.F., Toggweiler, J.R., Edwards, R.L., Schaefer, J.M., Putnam, A.E., 2010. The last glacial termination. Science 328 (June), 1652–1656. https://doi.org/10.1126/science.1184119.

DGA, 2022. Inventario Público de Glaciares (IPG2022). Dirección General de Aguas, Ministerio de Obras Públicas, Santiago, Chile.

Evans, I.S., 1977. World-wide variations in the direction and concentration of cirque and glacier aspects. Geogr. Ann. Ser. B 59 (3–4), 151–175. https://doi.org/10.1080/04353676.1977.11879949.

Evans, I.S., 2006a. Allometric development of glacial cirque form: Geological, relief and regional effects on the cirques of Wales. Geomorphology 80 (3–4), 245–266. https://doi.org/10.1016/j.geomorph.2006.02.013.

Evans, I.S., 2006b. Local aspect asymmetry of mountain glaciation: a global survey of consistency of favoured directions for glacier numbers and altitudes. Geomorphology 73 (1–2), 166–184. https://doi.org/10.1016/j.geomorph.2005.07.009.

Evans, I.S., Cox, N., 1974. Geomorphometry and the operational definition of cirques. Area 6 (2), 150–153.

Evans, I.S., Cox, N.J., 2017. Comparability of cirque size and shape measures between regions and between researchers. Zeitschrift Fur Geomorphologie 61, 81–103. https://doi.org/10.1127/zfg_suppl/2016/0329.

Falaschi, D., Lenzano, M.G., Villalba, R., Bolch, T., Rivera, A., Lo Vecchio, A., 2019. Six decades (1958–2018) of geodetic glacier mass balance in Monte San Lorenzo, Patagonian Andes. Front. Earth Sci. 7 (December). https://doi.org/10.3389/feart.2019.00326.

Federici, P.R., Spagnolo, M., 2004. Morphometric analysis on the size, shape and areal distribution of glacial cirques in the Maritime Alps (Western French-Italian Alps). Geogr. Ann. Ser. B 86 (3), 235–248. https://doi.org/10.1111/j.0435-3676.2004.00228.x.

Fick, S.E., Hijmans, R.J., 2017. WorldClim 2: new 1-km spatial resolution climate surfaces for global land areas. Int. J. Climatol. 37 (12), 4302–4315. https://doi.org/10.1002/joc.5086.

Garcia, J.L., 2012. Late Pleistocene ice fluctuations and glacial geomorphology of the Archipiélago de Chiloé, southern Chile. Geogr. Ann. Ser. B 94 (4), 459–479.

García, J.L., Hein, A.S., Binnie, S.A., Gómez, G.A., González, M.A., Dunai, T.J., 2018. The MIS 3 maximum of the Torres del Paine and Última Esperanza ice lobes in Patagonia and the pacing of southern mountain glaciation. Quaternary Science Reviews 185, 9–26. https://doi.org/10.1016/j.quascirev.2018.01.013.

García-Ruiz, J.M., Gómez-Villar, A., Ortigosa, L., Martí-Bono, C., 2000. Morphometry of glacial cirques in the central Spanish pyrenees. Geogr. Ann. Ser. B 82 (4), 433–442. https://doi.org/10.1111/j.0435-3676.2000.00132.x.

Garreaud, R., Lopez, P., Minvielle, M., Rojas, M., 2013. Large-scale control on the Patagonian climate. J. Climate 26 (1), 215–230. https://doi.org/10.1175/JCLI-D-12-00001.1.

Glasser, N., Jansson, K., 2008. The Glacial map of southern South America. J. Maps 4 (1), 175–196. https://doi.org/10.4113/jom.2008.1020.

Glasser, N.F., Jansson, K.N., Harrison, S., Kleman, J., 2008. The glacial geomorphology and Pleistocene history of South America between 38S and 56S. Quaternary Science Reviews 27 (3–4), 365–390. https://doi.org/10.1016/j.quascirev.2007.11.011.

Hall, Brenda L., Porter, C.T., Denton, G.H., Lowell, T.V., Bromley, G.R.M., 2013. Extensive recession of Cordillera Darwin glaciers in southernmost South America during Heinrich Stadial 1. Quaternary Science Reviews 62, 49–55. https://doi.org/10.1016/j.quascirev.2012.11.026.

Hall, B.L., Lowell, T.V., Bromley, G.R.M., Denton, G.H., Putnam, A.E., 2019. Holocene glacier fluctuations on the northern flank of Cordillera Darwin, southernmost South America. Quaternary Science Reviews 222. https://doi.org/10.1016/j.quascirev.2019.105904.

Herman, F., Brandon, M., 2015. Mid-latitude glacial erosion hotspot related to equatorial shifts in southern Westerlies. Geology 43 (11), 987–990. https://doi.org/10.1130/G37008.1.

Hubbard, A., Hein, A.S., Kaplan, M.R., Hultun, N.R.J., Glasser, N., 2005. A modelling reconstruction of the last glacial maximum ice sheet and its deglaciation in. Geogr. Ann. 87 (2), 375–391.

Hughes, P.D., Gibbard, P.L., Woodward, J.C., 2007. Geological controls on Pleistocene glaciation and cirque form in Greece. Geomorphology 88 (3–4), 242–253. https://doi.org/10.1016/j.geomorph.2006.11.008.

Hulton, N.R.J., Sugden, D.E., Payne, A.J., Clapperton, C.M., 1994. Glacier modeling and the climate of Patagonia during the last Glacial Maximum. Quatern. Res. 42, 1–19.

Ipsen, H.A., Principato, S.M., Grube, R.E., Lee, J.F., 2018. Spatial analysis of cirques from three regions of Iceland: implications for cirque formation and palaeoclimate. Boreas 47 (2), 565–576. https://doi.org/10.1111/bor.12295.

Křížek, M., Mida, P., 2013. The influence of aspect and altitude on the size, shape and spatial distribution of glacial cirques in the High Tatras (Slovakia, Poland). Geomorphology 198, 57–68. https://doi.org/10.1016/j.geomorph.2013.05.012.

Leger, T.P.M., Hein, A.S., Bingham, R.G., Martini, M.A., Soteres, R.L., Sagredo, E.A., Martínez, O.A., 2020. The glacial geomorphology of the Río Corcovado, Río Huemul and Lago Palena/General Vintter valleys, northeastern Patagonia (43°S, 71°W). J. Maps 16 (2), 651–668. https://doi.org/10.1080/17445647.2020.1794990.

Leger, T.P.M., Hein, A.S., Goldberg, D., Schimmelpfennig, I., Wyk, Van, de Vries, M.S., Bingham, R.G., 2021. Northeastern Patagonian Glacier advances (43°S) Reflect Northward Migration of the Southern Westerlies Towards the end of the last Glaciation. Front. Earth Science 9 (751987). https://doi.org/10.3389/feart.2021.751987.

Leger, T.P.M., Hein, A.S., Rodés, Á., Bingham, R.G., Schimmelpfennig, I., Fabel, D., Tapia, P., Aumaître, G., Zaidi, F., Keddadouche, K., 2023. A cosmogenic nuclide-derived chronology of pre-last Glacial Cycle glaciations during MIS 8 and MIS 6 in northern Patagonia. Clim. Past 19 (1), 35–59. https://doi.org/10.5194/cp-19-35-2023.

Li, Y., Zhao, Z., Evans, I.S., 2023. Cirque Morphology and Palaeo-climate Indications along a South-North Transect in High Mountain Asia. Geomorphology 431, 108688. https://doi.org/10.1016/j.geomorph.2023.108688.

Lizuaín, A., Panza, J.L.A., 2018. Mapa Geológico del Sector Continental e Insular Americano de la República Argentina - Mapa Geológico del Sector Antártico Argentino. Servicio Geológico Minero Argentino. Instituto de Geología y Recursos Minerales, Buenos Aires.

Lowell, T.V., Heusser, C.J., Andersen, B.G., Moreno, P.I., Hauser, A., Heusser, L.E., Schluchter, C., Marchant, D.R., Denton, G.H., 1995. Interhemispheric correlation of late pleistocene glacial events. Science 269 (5230), 1541–1549. https://doi.org/10.1126/science.269.5230.1541.

Menounos, B., Clague, J.J., Osborn, G., Davis, P.T., Ponce, F., Goehring, B., Maurer, M., Rabassa, J., Coronato, A., Marr, R., 2013. Latest Pleistocene and Holocene glacier fluctuations in southernmost Tierra del Fuego, Argentina. Quaternary Science Reviews 77, 70–79. https://doi.org/10.1016/j.quascirev.2013.07.008.

Mercer, J.H., Sutter, J.F., 1982. Late miocene-earliest pliocene glaciation in southern Argentina: implications for global ice-sheet history. Palaeogeography, Palaeoclimatology, Palaeoecology 38 (3–4), 185–206. https://doi.org/10.1016/0031-0182(82)90003-7.

Mîndrescu, M., Evans, I.S., Cox, N.J., 2010. Climatic implications of cirque distribution in the Romanian Carpathians: Palaeowind directions during glacial periods. J. Quat. Sci. 25 (6), 875–888. https://doi.org/10.1002/jqs.1363.

Moreno, P.I., Denton, G.H., Moreno, H., Lowell, T.V., Putnam, A.E., Kaplan, M.R., 2015. Radiocarbon chronology of the last glacial maximum and its termination in northwestern Patagonia. Quaternary Science Reviews 122, 233–249. https://doi.org/10.1016/j.quascirev.2015.05.027.

Moreno, P.I., Henríquez, W.I., Pesce, O.H., Henríquez, C.A., Fletcher, M.S., Garreaud, R. D., Villa-Martínez, R.P., 2021. An early Holocene westerly minimum in the southern mid-latitudes. Quaternary Science Reviews 251, 106730. https://doi.org/10.1016/j.quascirev.2020.106730.

Moreno, P.I., Fercovic, E.I., Soteres, R.L., Ugalde, P.I., Sagredo, E.A., Villa-Martínez, R.P., 2022. Glacier and terrestrial ecosystem evolution in the Chilotan archipelago sector of northwestern Patagonia since the last Glacial termination. Earth Sci. Rev. 235, 104240. https://doi.org/10.1016/j.earscirev.2022.104240.

Muir, R., Eaves, S., Vargo, L., Anderson, B., Mackintosh, A., Sagredo, E., Soteres, R., 2023. Late glacial climate evolution in the Patagonian Andes (44–47° S) from alpine glacier modelling. Quaternary Science Reviews 305, 108035. https://doi.org/10.1016/j.quascirev.2023.108035.

Oien, R.P., Spagnolo, M., Rea, B.R., Barr, I.D., Bingham, R.G., 2020. Climatic controls on the equilibrium-line altitudes of Scandinavian cirque glaciers. Geomorphology 352, 106986. https://doi.org/10.1016/j.geomorph.2019.106986.

Oien, R.P., Barr, I.D., Spagnolo, M., Bingham, R.G., Rea, B.R., Jansen, J., 2022. Controls on the altitude of Scandinavian cirques: what do they tell us about palaeoclimate? Palaeogeogr. Palaeoclimatol. Palaeoecol. 600, 111062. https://doi.org/10.1016/j.palaeo.2022.111062.

Oliva, L., Cioccale, M.A., Rabassa, J.O., 2020. Morphometry and spatial distribution of glacial cirques in the western Fuegian Andes of Argentina, southernmost South America. Andean Geol. 47 (2), 316–350. https://doi.org/10.5027/andgeov47n2-3188.

Pankhurst, R.J., Weaver, S.D., Hervé, F., Larrondo, P., 1999. Mesozoic-Cenozoic evolution of the North Patagonian Batholith in Aysen, southern Chile. J. Geol. Soc. London 156 (4), 673–694. https://doi.org/10.1144/gsjgs.156.4.0673.

Pedraza, J., Carrasco, R.M., Villa, J., Soteres, R.L., Karampaglidis, T., Fernández-Lozano, J., 2019. Cirques in the Sierra de Guadarrama and Somosierra Mountains (Iberian Central System): Shape, size and controlling factors. Geomorphology 341, 153–168. https://doi.org/10.1016/j.geomorph.2019.05.024.

Pellitero, R., Barr, I.D., Spagnolo, M., Tomkins, M., 2024. Morphometric analysis of cirques on the Iberian Peninsula provides insights into climate during past glaciations. Geomorphology 461, 109318. https://doi.org/10.1016/j.geomorph.2024.109318.

Peltier, C., Kaplan, M.R., Birkel, S.D., Soteres, R.L., Sagredo, E.A., Aravena, J.C., Araos, J., Moreno, P.I., Schwartz, R., Schaefer, J.M., 2021. The large MIS 4 and long MIS 2 glacier maxima on the southern tip of South America. Quaternary Science Reviews 262, 106858. https://doi.org/10.1016/j.quascirev.2021.106858.

Pérez-Flores, P., Cembrano, J., Sánchez-Alfaro, P., Veloso, E., Arancibia, G., Roquer, T., 2016. Tectonics, magmatism and paleo-fluid distribution in a strike-slip setting: Insights from the northern termination of the Liquiñe-Ofqui fault System, Chile. Tectonophysics 680, 192–210. https://doi.org/10.1016/j.tecto.2016.05.016.

Pérez-Peña, J.V., Al-Awabdeh, M., Azañón, J.M., Galve, J.P., Booth-Rea, G., Notti, D., 2017. SwathProfiler and NProfiler: two new ArcGIS Add-ins for the automatic extraction of swath and normalized river profiles. Comput. Geosci. 104, 135–150. https://doi.org/10.1016/j.cageo.2016.08.008.

Porter, S.C., 1977. Present and past glaciation threshold in the cascade range, Washington, U.S.A.: topographic and climatic controls, and paleoclimatic implications. J. Glaciol. 18 (78), 101–116. https://doi.org/10.3189/s0022143000021559.

Porter, S.C., 1989. Some geological implications of average Quaternary glacial conditions. Quatern. Res. 32 (3), 245–261. https://doi.org/10.1016/0033-5894(89)90092-6.

Porter, S.C., 2001. Snowline depression in the tropics during the last glaciation. Quat. Sci. Rev. 20, 1067–1091. https://doi.org/10.1016/S0277-3791(00)00178-5.

Principato, S.M., Lee, J.F., 2014. GIS analysis of cirques on Vestfirdir, Northwest Iceland: Implications for palaeoclimate. Boreas 43 (4), 807–817. https://doi.org/10.1111/bor.12075.

Rabassa, J., Coronato, A., Martínez, O., 2011. Late Cenozoic glaciations in Patagonia and Tierra del Fuego: an updated review. Biol. J. Linn. Soc. 103 (2), 316–335. https://doi.org/10.1111/j.1095-8312.2011.01681.x.

Rojas, M., Moreno, P., Kageyama, M., Crucifix, M., Hewitt, C., 2009. The Southern Westerlies during the last glacial maximum in PMIP2 simulations. Climate Dynam. https://doi.org/10.1007/s00382-008-0421-7.

Ruszkiczay-Rüdiger, Z., Kern, Z., Urdea, P., Madarász, B., Braucher, R., 2021. Limited glacial erosion during the last glaciation in mid-latitude cirques (Retezat Mts, Southern Carpathians, Romania). Geomorphology 384. https://doi.org/10.1016/j.geomorph.2021.107719.

Sagredo, E.A., Lowell, T.V., 2012. Climatology of Andean glaciers: a framework to understand glacier response to climate change. Global Planet. Change 86–87, 101–109. https://doi.org/10.1016/j.gloplacha.2012.02.010.

Sagredo, E.A., Rupper, S., Lowell, T.V., 2014. Sensitivities of the equilibrium line altitude to temperature and precipitation changes along the Andes. Quatern. Res. 81 (2), 355–366. https://doi.org/10.1016/j.yqres.2014.01.008.

Sagredo, E.A., Lowell, T.V., Kelly, M.A., Rupper, S., Aravena, J.C., Ward, D.J., Malone, A. G.O., 2017. Equilibrium line altitudes along the Andes during the last millennium: Paleoclimatic implications. Holocene 27 (7), 1019–1033. https://doi.org/10.1177/0959683616678458.

Sagredo, E.A., Kaplan, M.R., Araya, P.S., Lowell, T.V., Aravena, J.C., Moreno, P.I., Kelly, M.A., Schaefer, J.M., 2018. Trans-pacific glacial response to the Antarctic Cold Reversal in the southern mid-latitudes. Quaternary Science Reviews. https://doi.org/10.1016/j.quascirev.2018.01.011.

Schaefer, M., Fonseca, D., Farias-Barahona, D., Casassa, G., 2020. Surface energy fluxes on Chilean glaciers: measurements and models. Cryosphere 14, 2545–2565. https://doi.org/10.5194/tc-2019-51.

SERNAGEOMIN, 2003. Mapa Geológico de Chile: Versión Digital. Servicio Nacional de Geología y Minería, Publicación Digital, p. 4.

Simsek, M., Zeynel Ozturk, M., Yesilyurt, S., Utlu, M., 2023. Morphometric characteristics and paleogeographic implication of glacial cirques in Eastern Black Sea Mountains (Türkiye). Geomorphology 441, 108889. https://doi.org/10.1016/j.geomorph.2023.108889.

Singer, B.S., Moreno-Yaeger, P., Townsend, M., Huber, C., Cuzzone, J., Edwards, B.R., Romero, M., Orellana-Salazar, Y., Marcott, S.A., Breunig, R.E., Ferrier, K.L., Scholz, K., Coonin, A.N., Alloway, B.V., Tremblay, M.M., Stevens, S., Fustos-Toribio, I., Moreno, P.I., Vera, F., Amigo, A., 2024. New perspectives on ice forcing in continental arc magma plumbing systems. J. Volcanol. Geotherm. Res. 455, 108187. https://doi.org/10.1016/j.jvolgeores.2024.108187.

Soteres, R.L., Sagredo, E.A., Moreno, P.I., Lowell, T.V., Alloway, B.V., 2022a. Glacial geomorphology of the central and southern Chilotan Archipelago (42.2°S–43.5°S), northwestern Patagonia. J. Maps 1–17. https://doi.org/10.1080/17445647.2021.2008538.

Soteres, R.L., Sagredo, E.A., Kaplan, M.R., Martini, M.A., Moreno, P.I., Reynhout, S.A., Schwartz, R., Schaefer, J.M., 2022b. Glacier fluctuations in the northern Patagonian Andes (44°S) imply wind-modulated interhemispheric in-phase climate shifts during termination 1. Sci. Rep. 12 (1), 1–11. https://doi.org/10.1038/s41598-022-14921-4.

Soteres, R.L., Riquelme, F.M., Sagredo, E.A., Kaplan, M.R., 2023. (Paleo) glacier studies in Patagonia over the past decades (1976–2020): A bibliometric perspective based on the Web of Science. J. South Am. Earth Sci. 122, 104173. https://doi.org/10.1016/j.jsames.2022.104173.

Spagnolo, M., Pellitero, R., Barr, I.D., Ely, J.C., Pellicer, X.M., Rea, B.R., 2017. ACME, a GIS tool for automated cirque metric extraction. Geomorphology 278, 280–286. https://doi.org/10.1016/j.geomorph.2016.11.018.

Spagnolo, M., Rea, B.R., Barr, I., 2022. The (mis)conception of average Quaternary conditions. Quatern. Res. 105, 235–240. https://doi.org/10.1017/qua.2021.48.

Sugden, D.E., Hulton, N.R., Purves, R.S., 2002. Modelling the inception of the Patagonian icesheet. Quat. Int. 95, 55–64. https://doi.org/10.1016/S1040-6182(02)00027-7.

Thomson, S.N., Brandon, M.T., Tomkin, J.H., Reiners, P.W., Vásquez, C., Wilson, N.J., 2010. Glaciation as a destructive and constructive control on mountain building. Nature 467 (7313), 313–317. https://doi.org/10.1038/nature09365.

Wallick, K.N., Principato, S.M., 2020. Quantitative analyses of cirques on the Faroe Islands: evidence for time transgressive glacier occupation. Boreas 49 (4), 828–840. https://doi.org/10.1111/bor.12458.

Willett, C.D., Ma, K.F., Brandon, M.T., Hourigan, J.K., Christeleit, E.C., Shuster, D.L., 2020. Transient glacial incision in the Patagonian Andes from ~6 Ma to present. Sci. Adv. 6 (7), 1–10. https://doi.org/10.1126/sciadv.aay1641.

Yan, Q., Wei, T., Zhang, Z., 2022. Modeling the climate sensitivity of Patagonian glaciers and their responses to climatic change during the global last glacial maximum. Quaternary Science Reviews 288, 107582. https://doi.org/10.1016/j.quascirev.2022.107582.

Zhang, Q., Fu, P., Yi, C., Wang, N., Wang, Y., Capolongo, D., Zech, R., 2020. Palaeoglacial and palaeoenvironmental conditions of the Gangdise Mountains, southern Tibetan Plateau, as revealed by an ice-free cirque morphology analysis. Geomorphology 370, 107391. https://doi.org/10.1016/j.geomorph.2020.107391.

Zhang, Q., Dong, W., Dou, J., Dong, G., Zech, R., 2021. Cirques of the central Tibetan Plateau: Morphology and controlling factors. Palaeogeography, Palaeoclimatology, Palaeoecology 582, 110656. https://doi.org/10.1016/j.palaeo.2021.110656.